PHYSICAL REVIEW D **84,** 075015 (2011)

Revisiting no-scale supergravity inspired scenarios: Updated theoretical and phenomenological constraints

Amine Benhenni,[1,2] Jean-Loïc Kneur,[1,2] Gilbert Moultaka,[1,2] and Sean Bailly[3]

[1]*CNRS, Laboratoire Charles Coulomb UMR 5221, F-34095, Montpellier, France*

[2]*Université Montpellier 2, Laboratoire Charles Coulomb UMR 5221, F-34095, Montpellier, France*

[3]*Laboratoire de Physique Théorique LAPTH, Université de Savoie, CNRS (UMR 5108) 9 chemin de Bellevue, BP 110, F-74941 Annecy-Le-Vieux Cedex, France*

(Received 8 July 2011; published 18 October 2011)

We consider no-scale supergravity inspired scenarios, where the gravitino mass and related soft supersymmetry-breaking parameters are determined dynamically by radiative corrections to an essentially flat tree-level potential in the supersymmetry-breaking hidden sector. We examine the theoretical and phenomenological viability of such a mechanism, when including up-to-date calculations of the low-energy sparticle spectrum and taking into account the latest LHC results and other experimental constraints. We (re)emphasize the role of the scale-dependent vacuum energy contribution to the effective potential, in obtaining realistic no-scale electroweak minima, examining carefully the impact of boundary conditions and of variants of the minimization procedure. We also discuss and implement the B_0 (soft breaking Higgs mixing parameter) input boundary condition at high scale, therefore fixing $\tan\beta(B_0)$ at low scales. For general high-scale boundary conditions with $B_0, m_0, \cdots \neq 0$, our analysis provides theoretical correlations among the supersymmetric, soft, and vacuum energy parameters and related phenomenological consequences at the LHC. For instance, a zero vacuum energy at the grand unified theory scale would lead to a decoupled supersymmetric spectrum, together with a light standard-model-like Higgs boson at the electroweak scale. Given the experimental exclusion limits, a substantial class of the boundary conditions, and, in particular, the strict no-scale with $m_0 = A_0 = B_0 = 0$, are only compatible with a stau being the lightest Minimal Supersymmetric Standard Model particle. Then, an enlarged allowed parameter space emerges when assuming a gravitino lightest supersymmetric particle to account for the observed dark matter relic density.

DOI: 10.1103/PhysRevD.84.075015 PACS numbers: 12.60.Jv

I. INTRODUCTION

Supersymmetry (SUSY) has imposed itself as the most popular ''beyond-the-standard-model'' scenario for many good reasons. In addition to appealing extended symmetry principles, it has the potential to solve some of the problems raised by the standard model, even though it was not originally introduced for this purpose. It solves the hierarchy problem by protecting the scalar sector from unnaturally large radiative corrections, provided that the superpartners lie in the TeV range [1–4]. It also predicts the gauge coupling unification [5–8] at a high scale consistent with experimental constraints, and provides very plausible particle candidates for the dark matter [9–11]. Last but not least, the very structure of the Minimal Supersymmetric Standard Model (MSSM) (and of many nonminimal extensions) leads generically to the radiative electroweak symmetry breaking (REWSB) mechanism [12–15].

The remaining open questions concern mainly the precise mechanism underlying the supersymmetry breaking itself. Most present viable scenarios assume that a dynamical or spontaneous symmetry breaking occurs in a hidden sector. The supersymmetry breaking is then transmitted to the visible low-energy sector via different mechanisms depending on the models. One of the most popular such scenario is when supersymmetry breaking is transmitted essentially via the gravitational interaction, in the gravity-mediated models. In an unbroken supergravity (SUGRA) model [16–20], the graviton and its superpartner, the gravitino, both have a vanishing mass. Once supersymmetry is broken, only the gravitino gets a mass via the super-Higgs mechanism. Therefore, the breaking of local supersymmetry is directly linked to the nonvanishing gravitino mass. In a standard SUGRA scenario with a canonical Kähler potential, when SUSY breaking is communicated gravitationally to the visible sector, the soft parameters are roughly of the same order as $m_{3/2} \sim M_{\rm SUSY}^2/M_P$, itself expected to be of order the electroweak (EW) scale. In this way, one ends up with the correct hierarchy between the Planck scale M_P, the SUSY-breaking scale $M_{\rm SUSY}$, and the EW breaking scale $M_{\rm EW}$, although the requirement of the vanishing tree-level potential is somewhat *ad hoc*. In the no-scale models, the basic idea is that the vanishing of the tree-level potential in the hidden sector direction can be automatic for an appropriately chosen form of the Kähler potential. Moreover, the value of $m_{3/2}$ can be fixed dynamically by radiative correction stabilization, and is simply related to other soft SUSY-breaking parameters. This no-scale approach has emerged quite early [21,22], and since then it has been regularly claimed to be ruled out and resurrected

in different forms several times. However, in most of nowadays phenomenological studies, ''no-scale'' is often a name for just the specific and very restricted boundary conditions on the SUGRA parameters, namely $m_0 = A_0 = 0$, where m_0 and A_0 are, respectively, the universal grand unified theory (GUT) scale values of the scalar mass and trilinear soft SUSY-breaking parameters, or $B_0 = m_0 = A_0 = 0$ in the strict no-scale model (B_0 being the soft SUSY-breaking Higgs mass-mixing parameter). Although well known to the no-scale model aficionados, it is worth emphasizing here that an essential feature of the original no-scale program is the possible dynamical determination of the gravitino mass and other related soft SUSY-breaking parameters, that may be realized with the above boundary conditions but also possibly with more general SUGRA ones. More precisely, the basic framework [21] is to first assume a specific Kähler potential such that there exists a flat direction (moduli) at tree level, thus also ensuring automatically a (tree-level) vanishing cosmological constant. The SUSY-breaking order parameter is the gravitino mass but is not determined at the tree level, i.e. the gravitino mass is ''sliding.'' Then, the flatness of the potential can be lifted by (nongravitational) radiative corrections originating from the strong and electroweak sectors at the electroweak symmetry-breaking scale. These corrections may trigger, under appropriate circumstances, a nontrivial minimum of the potential as a function of the gravitino mass, thus fixing the latter. In principle, this picture does not forbid having weak quantum corrections to the vacuum energy, as long as those are of order $\sim m_{3/2}^4$ [23]. So, actually, one has rather an ''almost flat'' moduli direction of the Kähler potential. Overall, the mechanism is somewhat similar to the REWSB mechanism, but provides an even more direct (and calculable) link between the EW and SUSY-breaking scales. In this way, the no-scale scenario relates those two scales more dynamically, explaining naturally the hierarchy $m_{\mathrm{SUSY}} \ll M_P$. The vacuum thus corresponds to a minimum of the potential with respect to the two Higgs fields and a hidden sector field z, whose vacuum expectation values (vev) determine, respectively, the weak scale masses and the gravitino mass $m_{3/2}$. Thus, the occurrence of a minimum in the z direction is a consequence of the loop-improved effective potential at the EW scale where the tree-level flatness is lifted. For the whole picture to work, one must further assume that there are no stronger, purely gravitational (quantum) corrections near the Planck scale M_P, with dangerous vacuum energy contributions of the form $\Lambda^2 \mathrm{Tr} M^2$, where $\Lambda \sim \mathcal{O}(M_P)$ is an appropriate cutoff beyond which quantum gravitational effects are non-negligible, and M generically the relevant masses of the high-scale hidden sector. In fact, specific models compatible with the no-scale boundary conditions are known to avoid this problem [23,24]. On more phenomenological grounds, one may always assume that those issues will ultimately be solved by a fully consistent superstring framework, an assumption no more (nor less) problematic than the standard *minimal* SUGRA picture with (assumed) universal soft parameters at high scale.

On the one hand, most analyses in the past aiming to determine possible no-scale $m_{3/2}$ minima were conducted with definite approximations in the effective potential and sparticle spectrum calculations. Typically, those studies mostly used (one-loop) renormalization group evolution (RGE) analytical solutions restricted to low $\tan\beta$ values, and also typically neglecting the nondominant couplings, non-renormalization group (RG) radiative corrections, and other nondominant terms in the one-loop effective potential, etc., with the legitimate aim of determining (semi-)analytical solutions. On the other hand, the situation since those early days of no-scale models has drastically changed concerning the elaboration level of (s)particle spectra calculation, so that such approximations are hardly considered satisfactory nowadays. There have been of course numerous more recent studies of the viability of the minimal supergravity (mSUGRA) subspace defined by the specific no-scale initial conditions with more elaborate particle spectra calculations, and updated phenomenological constraints. However, most of those more recent studies are generally not addressing the existence of $V_{\mathrm{eff}}(m_{3/2})$ minima. Actually, to the best of our knowledge a systematic study of the occurrence of nontrivial no-scale $m_{3/2}$ minima of a well-defined (RG-improved) effective potential $V_{\mathrm{full}}(v_u, v_d; m_{3/2})$, taking into account its full one-loop radiative corrections, has not been done (though a number of special cases, other models, or partial studies of those aspects have been examined in the past or recently [25,26]). In addition, in spite of the above-mentioned superstring motivations and different appealing scenarios, in the following we will essentially consider a more phenomenological approach. More precisely, we shall consider the standard mSUGRA parameter models, with more specific boundary conditions like in the strict no-scale models, but also more general ones, for which we examine the conditions for the emergence of nontrivial $m_{3/2}$ minima at the EW scale. This is thus a ''no-scale inspired'' but more ''bottom-up'' framework, with the goal of determining what kind of high-scale parameter relations can emerge from our analysis.

The paper is organized as follows: Sec. II gives a short reminder of the basic no-scale supergravity scenario. In Sec. III, we specify our procedure for minimizing the loop-improved effective potential, examining some salient features to take into account. We emphasize, in particular, the role played in the $V_{\mathrm{eff}}(m_{3/2})$ minimization by the necessary scale-dependent vacuum energy contribution to the effective potential. This point was indeed raised earlier [27–29], and in fact our practical procedure is closely related to the latter work. (However, at the time those analyses used semianalytical approximations essentially similar to the

ones mentioned above, while we will perform more complete numerical studies based on the available present SUSY spectrum calculators.) In Sec. IV, we discuss in some detail important generic properties and results for the minimization of the loop-improved effective potential with respect to the extra soft breaking parameters. We emphasize also the differences in choice of $\tan\beta$ or B_0 as input parameter, the latter being the consistent choice in no-scale scenarios, which has nontrivial technical as well as phenomenological consequences. Section V examines a few different representative parameter cases, either in the strict no-scale models or its generalizations, and following well-defined prescriptions for a loop-improved effective potential. The main phenomenological constraints affecting the viability of the theoretical results when confronted with collider and other experimental limits are illustrated. We also explore the constraints given by the dark matter relic density, either in the standard neutralino lightest supersymmetric particle (LSP) scenario, or considering alternatively that the LSP is the gravitino, which can be *a priori* assumed in a generalized no-scale scenario. Finally, we give some conclusions in Sec. VI.

II. BASICS OF NO-SCALE SUPERGRAVITY

For completeness, we review very sketchily in this section the essential features of the original no-scale models, referring for more details to the pioneering literature [21,22,30]. The $N = 1$ supergravity Lagrangian is fully determined by the Kähler potential and superpotential. For simplicity, we focus here only on the matter chiral superfield dependence (referring only implicitly to the gauge vector superfields and gravitino supermultiplet sectors). The gauge kinetic function $f_{ab}(\phi_i)$, the Kähler potential $K(\phi_i, \bar{\phi}_i)$, and the superpotential $W(\phi_i)$ are specified in terms of the chiral superfields ϕ_i and their complex conjugate $\bar{\phi}_i$. Here, ϕ_i denotes generically all visible and hidden sector superfields, possibly transforming under some gauge groups. In terms of the Kähler function

$$G(\phi_i, \bar{\phi}_i) = \frac{K(\phi_i, \bar{\phi}_i)}{m_p^2} + \ln\frac{|W(\phi_i)|^2}{m_p^6}, \tag{2.1}$$

where m_p is the reduced Planck scale $m_p \equiv M_P/\sqrt{8\pi}$, one obtains the F-term part of the scalar potential

$$V_F = m_p^4 e^G (G_i G^{i\bar{j}} G_{\bar{j}} - 3), \tag{2.2}$$

where

$$G_i \equiv \frac{\partial G}{\partial \phi_i}, \quad G_{\bar{i}} \equiv \frac{\partial G}{\partial \bar{\phi}_i}, \quad G_{i\bar{j}} \equiv \frac{\partial^2 G}{\partial \phi_i \partial \bar{\phi}_j}, \quad G^{i\bar{j}} \equiv (G^{-1})_{i\bar{j}}. \tag{2.3}$$

Because of local supersymmetry, the vacuum energy deduced from (2.2) is in general nonvanishing even before SUSY breaking. After SUSY breaking, the gravitino acquires a mass $m_{3/2}$ given by

$$m_{3/2} = m_p e^{\langle G\rangle/2}, \tag{2.4}$$

where $\langle G\rangle$ is a function of the vevs of the scalar components of a subclass ϕ_k of the chiral superfields responsible for the SUSY breaking, whatever the underlying breaking mechanism may be. The corresponding nonvanishing F-term vevs $F_k = m_p^3\langle e^{G/2} G_k\rangle$ yield the SUSY-breaking mass scale

$$M_{\rm SUSY} = (F_k G^{k\bar{j}} F_{\bar{j}})^{1/4}. \tag{2.5}$$

Fine-tuning $\langle V_F\rangle$ to 0 to keep the (tree-level) cosmological constant around its observed value fixes $\langle G_k G^k\rangle$ uniquely, leading to the well-known relation

$$m_{3/2} = \frac{M_{\rm SUSY}^2}{\sqrt{3} m_p}. \tag{2.6}$$

If SUSY breaking is communicated gravitationally to the visible sector, one expects *generically* the soft parameters $m_{\rm soft}$ to satisfy

$$m_{\rm soft} = \mathcal{O}(1) \times m_{3/2} \tag{2.7}$$

and $m_{3/2}$ not far from the electroweak scale. Moreover, the generic magnitude $\langle V_F\rangle \sim \mathcal{O}(m_{3/2}^2 m_p^2)$ [see (2.2) and (2.4)] exacerbates the fine-tuning of the vacuum energy to zero for $m_{3/2}$ of order the EW scale. No-scale supergravity [21,22,31] was introduced to ensure naturally, through a suitable choice of the Kähler potential, a vanishing potential at the tree level in the hidden sector scalar fields directions at every value of these fields. Since on the one hand the $\mathcal{O}(m_{3/2}^2 m_p^2)$ magnitude in V_F is now flattened, and on the other the vevs of the hidden sector fields, and thus $m_{3/2}$, are undetermined at the tree level, $m_{3/2}$ will be fixed at the loop level through (generalized) REWSB, which takes place in the observable sector, with $m_{3/2} \sim \mathcal{O}(m_Z)$ as a natural outcome. This holds only if a large mass scale M that can be present in the observable sector, such as a GUT scale, does not contribute to the potential by quantities of $\mathcal{O}(m_{3/2}^2 M^2)$.

Assuming for simplicity that the hidden sector contains only one chiral superfield z (say ϕ_1 of the above set of ϕ_i's), the simplest Kähler potential realizing the above potential flatness, entailing a (noncompact) $SU(1, 1)$ symmetry, is given by

$$K = -3\ln(z + \bar{z}). \tag{2.8}$$

This Kähler potential has to be supplemented in realistic models by other Kähler potential and superpotential parts depending on the visible sector fields. A generalization of the corresponding Kähler function $G(z, \phi_k)$,

$$G = -\frac{3}{m_p^2}\ln(z + \bar{z} - f(\phi_k, \bar{\phi}_k)) + \ln\frac{|W(\phi_k)|^2}{m_p^6}, \tag{2.9}$$

where the ϕ_k's (with $k \geq 2$) are all in the visible sector, was found to have very nice properties, either (i) when f is an arbitrary function but W trivial (e.g. $W = m_p^3$), or (ii) when W is an arbitrary superpotential (e.g. that of the

MSSM or of an extended GUT model) but f taking the special form $f(\phi_k, \bar{\phi}_k) = \sum_{k\geq 2}|\phi_k|^2$. In case (ii), the $SU(1, 1)$ symmetry of (2.8) is extended to $SU(n, 1)$, where $n-1$ is the number of fields in the observable sector. A key point for both (i) and (ii) cases is that SUSY breaking in the hidden sector leaves the visible chiral superfield sector supersymmetric. This is welcome particularly in case (ii), where a full GUT sector can be accommodated, including the MSSM as the low-energy effective theory, since the nontransmission of SUSY breaking will protect the visible sector from the large $\mathcal{O}(m_{3/2}^2 M_{\rm GUT}^2)$ effects mentioned previously. However, for the same reason contributions $\mathcal{O}(m_{3/2}^2 m_W^2)$ will not be present either, thus preventing the usual radiative EW symmetry breaking and the ensuing dynamical determination of $m_{3/2}$. All soft breaking squark, slepton, and Higgs masses and couplings are thus vanishing at all scales, and, in particular, the universal parameters at the GUT scale,

$$m_0 = A_0 = B_0 = 0. \tag{2.10}$$

The only source left for SUSY breaking is in the gauge/gaugino sector through the inclusion of z-field-dependent noncanonical gauge kinetic functions $f_{ab}(z, \ldots)$, which are essentially free in a general supergravity framework [16–20]. The ensuing soft breaking gaugino mass terms take then the form $\frac{1}{4} m_{3/2} \langle G_{\bar{z}}/G_{\bar{z}\bar{z}} \partial f_{ab}/\partial z\rangle$. One should still assume that f_{ab} is chosen such that the heavy GUT gaugino soft masses remain vanishing so that again large unwanted contributions $\mathcal{O}(m_{3/2}^2 M_{\rm GUT}^2)$ are not present. The remaining MSSM gaugino masses are proportional to $m_{3/2}$ as just noted. Within the universal gaugino mass assumption, we rewrite this relation for later phenomenological use at the GUT scale as

$$m_{3/2} = c_{3/2} m_{1/2}. \tag{2.11}$$

Equations (2.10) and (2.11) define the boundary conditions of the strict no-scale scenario. It is now possible to imagine variants to these boundary conditions. For instance, supplementing case (i) with a superpotential in the visible sector implies a nonvanishing A_0. Another variant is to consider $B_0 \neq 0$ keeping the boundary conditions

$$m_0 = A_0 = 0. \tag{2.12}$$

Analogous relations arise naturally in low-energy effective models for some specific string theories [23,32,33], leading to generalized boundary conditions depending on the type of the string and the compactification mechanism. For instance, in the dilaton-dominated SUSY-breaking scenario, the conditions become

$$m_0 = \frac{1}{\sqrt{3}} m_{1/2}, \qquad A_0 = -m_{1/2}, \qquad B_0 = \frac{2}{\sqrt{3}} m_{1/2}, \qquad m_{1/2} = \sqrt{3} m_{3/2}, \tag{2.13}$$

with thus nonzero values of m_0, B_0, and other high-scale parameters, but all related to the unique SUSY-breaking scale, $\sim m_{1/2}$. In contrast, note that the strict no-scale relations in Eq. (2.10) are equivalent to the so-called moduli-dominated SUSY-breaking superstring model. It is now possible to study the electroweak potential and to predict values for $m_{1/2}$ instead of $m_{3/2}$ by an extra minimization in addition to the ordinary EW minimization driven by the REWSB mechanism. Using a simplified analysis with approximations allowing analytical handling of expressions [21,22], the preferred values appeared to be of order

$$m_{1/2} \sim \mathcal{O}(m_{3/2}) \sim \mathcal{O}(m_Z). \tag{2.14}$$

As mentioned before, strict no-scale supergravity is characterized by the specific boundary conditions at GUT scale given by Eq. (2.10). We are left with only $m_{1/2}$ as a free parameter, parameterizing the supersymmetry breaking, and driving the other parameters through renormalization group evolution (RGE) effects.

In the following, we consider a more phenomenological approach, essentially string-model-independent, motivated by the fact that the ultimate superstring framework, and even more how it is linked to the GUT scale, is not yet fully established. We will thus assume the most general standard mSUGRA high-scale parameters and boundary conditions, but study also the special cases of no-scale (2.12) and strict no-scale models (2.10). This more phenomenological approach aims to concentrate more on the conditions for the emergence of a third nontrivial minimum of $V_{\rm eff}$ with respect to $m_{1/2}$ at the EW scale, without too-strong prejudice on the high-scale models. We will assume the following generic form of the boundary conditions

$$B_0 = b_0 m_{1/2}, \quad m_0 = x_0 m_{1/2}, \quad A_0 = a_0 m_{1/2}, \tag{2.15}$$

where b_0, a_0, x_0 are mass-independent constants taken as input parameters. Further input information about the supersymmetric μ parameter is also needed, even though the value of μ at the electroweak scale will be as usual eventually fixed (up to a sign) by the REWSB conditions. Indeed, since $m_{1/2}$ will be determined dynamically from the potential, it is important to know beforehand whether μ has a functional dependence on $m_{1/2}$, for instance through its boundary value μ_0 at the high scale. For reasons which will become clear in the sequel, we will adopt throughout the paper the boundary condition

$$\mu_0 = c_\mu^0 m_{1/2}, \tag{2.16}$$

with c_μ^0 an independent constant. Although μ is a supersymmetric parameter, such an assumption is well motivated as there are various mechanisms where it can be related to the SUSY-breaking order parameter $m_{3/2}$ within supergravity. Typically, this can occur through a nonminimal term in the Kähler potential involving the two Higgs

superfields and some gauge singlet superfield whose F-term triggers supersymmetry [34,35], or alternatively through a minimal term in the Kähler potential and the addition of an R-symmetry breaking constant in the superpotential [36], (see also for instance [37] for an early review of other possible mechanisms including the superstring induced ones).

We close this section by stressing that the usual free parameters of mSUGRA $(m_0, m_{1/2}, A_0, \tan\beta, \mathrm{sign}(\mu))$ have been traded here for b_0, a_0, x_0, and (sign of) c^0_μ, thus with one less free parameter, $m_{1/2}$, to be determined dynamically, hence a more constrained scenario. Furthermore, in the spirit of no-scale, the dimensionless parameters b_0, a_0, x_0, and c^0_μ are expected to be of $\mathcal{O}(1)$, or else strictly vanishing. These features are useful criteria distinguishing the no-scale scenario from the less-constrained mSUGRA, even if both can lead to similar low-energy MSSM spectra.

III. PRESENT SITUATION VS EARLY NO-SCALE MODEL ANALYSIS

In this section, we first review some rather generic and important features of the no-scale mechanism, by which a dynamical determination of the soft parameters is provided via the extra minimization of the effective potential. Consider the familiar MSSM effective potential, for the moment just at tree level for simplicity, which reads

$$V_{\mathrm{tree}} = m_1^2|H_u|^2 + m_2^2|H_d|^2 - B\mu H_u.H_d + \frac{g^2+g'^2}{8}(|H_u|^2 - |H_d|^2)^2 \tag{3.1}$$

in the relevant electrically neutral Higgs field directions

$$H_u^0 = \begin{pmatrix} 0 \\ h_u \end{pmatrix} \qquad H_d^0 = \begin{pmatrix} h_d \\ 0 \end{pmatrix}, \tag{3.2}$$

where $m_1^2 \equiv m_{H_u}^2 + \mu^2$, $m_2^2 \equiv m_{H_d}^2 + \mu^2$, g, g' denote, respectively, the $SU(2)_L$ and $U(1)_Y$ gauge couplings and the "." denotes the $SU(2)$ scalar product. Once the EW symmetry breaking mechanism occurs, the Higgs fields develop nonvanishing vacuum expectation values $\langle h_u\rangle = v_u$, $\langle h_d\rangle = v_d$, and the EW extremum is characterized by

$$\frac{\partial V}{\partial H_u|_i}\Big|_{H_u=\langle H_u^0\rangle, H_d=\langle H_d^0\rangle} = 0, \qquad \frac{\partial V}{\partial H_d|_i}\Big|_{H_u=\langle H_u^0\rangle, H_d=\langle H_d^0\rangle} = 0, \tag{3.3}$$

where $i = 1, \ldots 4$ runs over the four field components of the H_u and H_d doublets, of which only the two conditions

$$\frac{\partial V}{\partial h_u} = 0, \qquad \frac{\partial V}{\partial h_d} = 0, \tag{3.4}$$

are not trivially satisfied, and allow to determine v_d and v_u in terms of m_1^2, m_2^2, $B\mu$, and $g^2 + g'^2$. Since the gauge invariant point $v_d = v_u = 0$ is also a solution of (3.4), one should require the consistency condition

$$m_1^2 m_2^2 \leq (B\mu)^2 \tag{3.5}$$

to assure that this point is not a minimum so that the electroweak symmetry is indeed broken. Note that one has to require as well

$$m_1^2 + m_2^2 \geq 2|B\mu| \tag{3.6}$$

to guarantee the tree-level stability of the potential.[1] Of course, one should further consider one-loop (and possible higher-order) corrections to the effective potential and other related radiative corrections to the sparticle masses without which the simple tree-level analysis is not sufficiently reliable. Now, essentially, the main additional feature of no-scale models is to seek for an extra nontrivial minimum:

$$\frac{\partial V}{\partial m_{3/2}} = 0, \tag{3.7}$$

or with $m_{3/2}$ replaced by $m_{1/2}$ in the above described case of a unique SUSY-breaking scale that can be conveniently parameterized in terms of $m_{1/2}$, as discussed in the previous section. The parameters in Eq. (3.1) depend nontrivially on $m_{1/2}$ via the high-scale boundary conditions, and follow RGE from high-scale values e.g. m_1(GUT) down to m_1(EW) values at the EW scale, where the minimization Eqs. (3.4) and (3.7) are required. Before examining in more detail the extra minimization (3.7), let us first examine some important aspects in defining the actual expression for the effective potential to be minimized. As mentioned before, in the early days of no-scale model analyses [21,22] or even a bit more recently [27–29], a number of approximations were used in order to get analytic expressions with a rather transparent picture for the behavior of the effective potential and its possible minima. While those approximations were legitimate at the time, clearly the situation will change substantially with an up-to-date analysis, potentially affecting the existence and location of possible $m_{1/2}$ minima of the effective potential. We list below some of the important features to be taken into account. Rather than giving somewhat blind final results, we find it instructive to disentangle and discuss the different (tree-level, loop-level) contributions as much as possible in order to pinpoint what contributions are

[1] There are connections between these two consistency conditions. If (3.5) is violated then (3.6) is necessarily fulfilled. This implies that the scale at which REWSB occurs is always higher than the scale at which the potential becomes unstable. Furthermore, when (3.6) is satisfied together with (3.4) then the REWSB extremum is guaranteed to be a minimum and (3.5) is automatically satisfied. These connections are typical of the MSSM Higgs sector potential and are not valid in a general two-Higgs doublet model. They are also modified by loop corrections to the effective potential [38].

actually responsible for the occurrence of nontrivial $m_{1/2}$ minima.

(i) Perhaps the most relevant point concerns the RG invariance of the effective potential: in principle, one would expect that the existence of minima is not strongly dependent on the choice of the EW and renormalization scales. However, this is a nontrivial issue since even the one-loop improved effective potential for the MSSM exhibits a rather important scale dependence in general, due to its intrinsic non-RG invariance unless one subtracts a scale-dependent vacuum-energy-like term. Although the necessity of including in general such a term was established since the work in Refs. [39–42], we stress that it has a drastic influence on the specific $m_{1/2}$ minimization results, as was indeed pointed out earlier in Refs. [27–29]. This will deserve a more detailed discussion below.

(ii) In the standard REWSB mechanism, the occurrence of a nontrivial EW minimum at some scale $Q_{\rm EW}$ is strongly determined by the driving of $m^2_{H_u}$ towards its EW scale value, characterized (very roughly) by $m^2_{H_u}(Q_{\rm EW}) < 0$. Indeed, the (one-loop) RGE for m_{H_u} reads:

$$8\pi^2 \frac{d}{d\ln Q} m^2_{H_u} = 3Y_t^2(m^2_{Hu} + m^2_{\tilde{Q}_L} + m^2_{\tilde{t}_R} + A_t^2) - g'^2 M_1^2 - 3g^2 M_2^2, \tag{3.8}$$

where for sufficiently large Y_t the first term on the right-hand side (RHS) largely dominates. (Note that the trace term "$TrYm^2$" is absent since we assumed mSUGRA boundary conditions at the GUT scale.) One might expect similarly that the occurrence of a nontrivial extra minimum of $V_{\rm eff}(m_{1/2})$ resembles the REWSB mechanism, therefore relying mostly as a first approximation on the running properties and $m_{1/2}$ dependence of the relevant Higgs sector parameters entering (3.1). This is, however, not the case, the detailed mechanism triggering possible $m_{1/2}$ minima being quite more subtle: within the initial conditions (2.15) and (2.16) and even when including the RGE running of the tree-level potential parameters, (3.1) does not lead to nontrivial $m_{1/2}$ extrema satisfying simultaneously (3.4) and (3.7), (except possibly at $m_{1/2} = 0$, but where the extremum is a maximum). Adding merely a vacuum energy term will already allow for local $m_{1/2}$ minima. More generally, as we shall examine later on, the occurrence of (phenomenologically relevant) nontrivial $m_{1/2}$ minima will result from the interplay between (3.1), the vacuum energy term, *and* the one-loop corrections to the effective potential.

(iii) Further influence on the precise location of $m_{1/2}$ minima comes from the necessary nonlogarithmic radiative corrections to (s)particle masses, i.e. that are not determined only from RG properties and can indirectly affect the effective potential dependence on $m_{1/2}$. Among those are the field-dependent contributions coming from the one-loop part of the effective potential, most conveniently included, at the EW minima, in the form of tadpole contributions [43]. Though these are naively reasonably moderate corrections with respect to a tree-level analysis, they can have in fact a strong influence on some crucial relations such as those involving μ, $m^2_{H_i}$, and the m_Z mass at the EW minimum. As a result, their global effect may shift substantially the $m_{1/2}$ minima with respect to a simple tree-level analysis. In addition, other non-RG radiative corrections are important especially for the top and bottom Yukawa couplings and (to a lesser extent) for the gauge couplings. For example, in the standard procedure where the top (pole) mass is input, one extracts the Yukawa coupling values at some chosen input scale $Q_{\rm in}$ (typically m_Z or EW) from the relation

$$m_{\rm top}^{\rm pole} = Y_t(Q_{\rm in})v_u(Q_{\rm in})(1 + \delta_y^{\rm RC}(Q_{\rm in}) + \cdots). \tag{3.9}$$

Here, the one-loop nonlogarithmic (SUSY and SM) corrections $\delta_y^{\rm RC}$ relate the pole mass to the running mass, and the ellipsis stands for higher-order corrections. Now, the supersymmetric and standard model contributions to $\delta_y^{\rm RC}$ are quite large and positive in most of the mSUGRA parameter space, such that the extracted value of $Y_t(Q_{\rm EW})$ is substantially smaller than what it would be in a pure RGE approximation neglecting $\delta_y^{\rm RC}$. Then, the precise value of Y_t has an important impact on the $m^2_{H_u}$ running among other things, thus also on the subsequent determination of other relevant parameters B, μ via the EW constraints. This emphasizes the importance of controlling all sources of radiative corrections for a better determination of the no-scale $m_{1/2}(m_{3/2})$ minima.

(iv) Finally there are other minor differences between up-to-date standard SUSY spectrum calculations and the above-mentioned approximations, like the fact that the RGEs are solved numerically for any $\tan\beta$, rather than analytically for a restricted range of small $\tan\beta$ values. In the following, we also mainly examine the influence of considering consistently the soft breaking Higgs mixing parameter, B_0, to be an input at the high scale, which is quite different from considering $\tan\beta \equiv v_u/v_d$ input (at low scale).

A. RG invariance and the effective potential

The tree-level potential (3.1) is known to have in general an unwelcome scale dependence. A first step to improve this situation is to consider the one-loop improved effective potential [44] defined in the $\overline{DR}'$ scheme [45,46] as

$$V_{\rm eff} \equiv V_{\rm tree} + V_{\text{1-loop}} = V_{\rm tree}[H_u, H_d](Q) + \frac{1}{64\pi^2}\sum_n (-1)^{2n} M_n^4(H_u, H_d) \times \left(\ln\frac{M_n^2(H_u, H_d)}{Q^2} - \frac{3}{2}\right), \tag{3.10}$$

where M_n are (field-dependent) mass eigenvalues and the summation runs over all (s)particle species and possible degeneracies due to color, flavor, etc. In the general MSSM, the one-loop term in (3.10) takes explicitly the form[2]

$$V_{\text{1-loop}} = \sum_{\phi^0} h(\phi^0) + 2\sum_{\phi^+} h(\phi^+) + 2\sum_{\tilde f} h(\tilde f) - 2\sum_{i=1,\ldots 4} h(N_i) - 4\sum_{i=1,2} h(C_i) - 16h(\tilde g) - 12(h(t) + h(b)) - 4h(\tau) + 3h(Z) + 6h(W) \tag{3.11}$$

in the notations of [45], where the name of each particle denotes its squared (field-dependent) mass and

$$h(x) \equiv \frac{x^2}{64\pi^2}\left(\ln\frac{x}{Q^2} - \frac{3}{2}\right). \tag{3.12}$$

The expression of RG invariance is formally

$$\left[\frac{\partial}{\partial \ln Q} + \sum_i \beta_i(\lambda_i)\frac{\partial}{\partial \lambda_i} - \gamma_{H_u} v_u \frac{\partial}{\partial v_u} - \gamma_{H_d} v_d \frac{\partial}{\partial v_d}\right] V_{\rm eff} = 0, \tag{3.13}$$

where λ_i designates generically all relevant couplings or masses, with β_i their corresponding beta functions, and γ_{H_i} are the anomalous dimensions of the Higgs fields. As is well known, the practical cancellations of scale dependence implied by RG invariance generally occurs among terms of different perturbative orders. Thus, the (one-loop level) cancellation of the scale dependence would be expected to occur between the relevant one-loop beta functions parts in Eq. (3.13) acting on the tree-level parameters in $V_{\rm tree}$ and the explicit Q dependence in the one-loop term above, up to higher-order (two-loop) remnant terms. However, in general in the presence of massive fields, and, in particular, in the MSSM due to the SUSY-breaking terms, this does not work so because the effective potential in the form (3.10) is not a proper RG-invariant physical quantity, so that there are remnant terms of one-loop order that do not cancel. Perhaps rather curiously, apart from early hints [47] this fact was not fully appreciated until the early nineties, where different detailed prescriptions were proposed [39–42], all pointing out the necessity to include a "vacuum energy" piece in addition to the above one-loop effective potential (3.10). One simple prescription is to subtract the field-independent zero-point (vacuum) energy [42]:

$$V_{\rm full} \equiv V_{\rm tree} + V_{\text{1-loop}} - V_{\text{1-loop,sub}} \tag{3.14}$$

with

$$V_{\text{1-loop,sub}} \equiv V_{\text{1-loop}}(H_u, H_d = 0), \tag{3.15}$$

which can easily be shown to have the same one-loop RG running as the remnant part from Eq. (3.10), therefore cancelling the scale dependence in the latter up to higher (two-loop) order terms. This subtraction is by construction similar to the supertrace in Eq. (3.10) but with a spectrum involving only soft terms and the supersymmetric μ parameter.[3] However, this subtraction is only one possible prescription, sufficient for RG invariance properties at this one-loop order, but having some limitations and unwelcome features [42], such as that the subtracted potential may become complex[4] A more general convenient prescription consists in adding a running vacuum energy to the potential:

$$V_{\rm full} \equiv V_{\rm tree}(Q) + V_{\text{1-loop}}(Q) + \tilde\Lambda_{\rm vac}(Q), \tag{3.16}$$

where the running of $\tilde\Lambda_{\rm vac}$ is determined by requiring $V_{\rm full}$ to satisfy (3.13), which leads to the (one-loop) RGE equation,

$$Q\frac{d}{dQ}\tilde\Lambda_{\rm vac}(Q) = \frac{1}{32\pi^2}\sum_n (-1)^{2n} M_n^4(H_u, H_d = 0). \tag{3.17}$$

A reasonably tractable expression at the two-loop level is also available [45]. The RGE of $\tilde\Lambda_{\rm vac}(Q)$ has no direct influence on other RG parameters, and $\tilde\Lambda_{\rm vac}(Q)$ behaves at the one-loop level qualitatively exactly like the above defined subtraction $V_{\text{1-loop,sub}}$, thus canceling the remnant non-RG-invariant terms from $V_{\rm tree} + V_{\rm loop}$ in (3.10).

[2]One should in principle also include in (3.11) the one-loop contribution of the gravitino, $-4h(\tilde G_{3/2})$. This contribution makes, however, very little numerical differences in our analysis, at least as long as $m_{3/2} \lesssim m_{1/2}$, since it has a rather small weight relative to the total sum over all contributions to (3.11). For generic input values and $m_{3/2} = m_{1/2}$, it is typically an $\mathcal{O}(1\%)$ effect.

[3]For $v_u = v_d = 0$, all particle masses originating from EW symmetry breaking are thus vanishing. The chargino and neutralino masses are respectively $|M_2|$, $|\mu|$, and $|M_1|$, $|M_2|$, $|\mu|$ with two degenerate ones. Similarly, the sfermion and scalar sector eigenmasses depend only on the soft terms and the μ parameter.

[4]This happens, in particular, in the MSSM case, where for $v_u = v_d = 0$ the (would be lightest) neutral and charged Higgs states become tachyonic whenever the REWSB conditions (3.5) are satisfied. Note, however, that these problems may be avoided by subtracting at other values of the Higgs fields.

Moreover, the running $\tilde{\Lambda}_{\rm vac}(Q)$ will be uniquely fixed once a choice is made of its boundary value at some arbitrary initial scale. In view of later discussions where the boundary conditions (2.15) and (2.16) will be assumed, we adopted here a notation with the tilde to indicate that the boundary value $\tilde{\Lambda}^0_{\rm vac}$ can be in principle quite general, including the possibility that the dimensionless quantity $\tilde{\Lambda}^0_{\rm vac}/m^4_{1/2}$ be $m_{1/2}$ *dependent*, while a Λ without a tilde will implicitly indicate that the boundary conditions $\Lambda^0_{\rm vac}/m^4_{1/2}$ are chosen $m_{1/2}$ ($m_{3/2}$) *independent*. We will refer to the latter as the "untwiddled prescription." This distinction is important insofar as we are interested in the minima of the potential with respect to $m_{1/2}$, given that one can always add to $\tilde{\Lambda}_{\rm vac}(Q)$ any arbitrary Q-independent function of $m_{1/2}$ without altering the RGE properties while modifying the structure of the $m_{1/2}$ minima. Throughout the paper, we adopt mainly the untwiddled prescription version of Eq. (3.16), but also occasionally illustrate the subtraction prescription (3.14), in particular, in Sec. IV E. Obviously, the latter prescription is but a special case of the general twiddled prescription (3.16), and (3.15) a special solution of the RGE (3.17) with a specific boundary condition at some scale $Q = Q_0$. Indeed, taking

$$\tilde{\Lambda}^{\,0}_{\rm vac} = -V_{1-{\rm loop,sub}}(H_u, H_d = 0, Q_0) \tag{3.18}$$

as a boundary condition ensures through (3.17) that

$$\tilde{\Lambda}_{\rm vac}(Q) = -V_{1-{\rm loop,sub}}(H_u, H_d = 0, Q) \tag{3.19}$$

for all Q. It is also obvious from the form of $V_{1-{\rm loop,sub}}$ that the boundary condition (3.18) is of the twiddled type, i.e. $\tilde{\Lambda}^0_{\rm vac}/m^4_{1/2}$ is a function of $m_{1/2}$ when (2.15) and (2.16) are assumed. It will prove phenomenologically useful to compare the subtraction prescription (3.14) and (3.15) with the untwiddled prescription of (3.16). Clearly, these are two different prescriptions from the point of view of no-scale, since they differ in the $m_{1/2}$ dependence of the boundary conditions, and thus lead to different $V_{\rm full}(m_{1/2})$ potentials.

The vacuum energy, being field independent by definition, has no influence on the EW minimization of the effective potential, Eq. (3.4), so that it can be safely omitted in all related issues. But, it can have a definite influence on the fate of eventual $V(m_{1/2})$ minima, contributing nontrivially to Eq. (3.7), as we will see in more detail later on. In a top-down approach, the running vacuum energy allows us to choose different boundary conditions for $\tilde{\Lambda}_{\rm vac}(Q)$. In particular, we shall consider different choices of $\tilde{\Lambda}_{\rm vac}(Q_{\rm GUT})$ or $\tilde{\Lambda}_{\rm vac}(Q_{\rm EW})$ and explore the consequences on the existence of $m_{1/2}$ minima for the full effective potential. This point was already noted and studied earlier [27–29], as mentioned in the introduction, but those studies relied on semianalytical expressions within approximations similar to the ones mentioned above. Following these authors, we parameterize the vacuum energy contribution at an arbitrary scale Q in terms of $m_{1/2}$ (or equivalently $m_{3/2}$), in the most general twiddled context, as

$$\tilde{\Lambda}_{\rm vac}(Q) \equiv \tilde{\eta}(Q) m^4_{1/2}, \tag{3.20}$$

where the running of $\tilde{\eta}(Q)$ at one-loop is determined by Eq. (3.17) together with the boundary condition defined e.g. at the GUT scale as $\tilde{\eta}(Q_{\rm GUT}) \equiv \tilde{\eta}_0$. We stress here that, on top of the $Q_{\rm GUT}$ dependence, $\tilde{\eta}(Q)$ can in general depend also on $m_{1/2}$ (or equivalently $m_{3/2}$). [We will come back to this point later on when discussing Eq. (4.5).]

The improvement in scale (in)dependence of $V_{\rm full}$ (3.16), as compared to $V_{\rm tree} + V_{\rm loop}$ alone, is illustrated in Fig. 1 for both the untwiddled prescription with $m_{1/2}$-independent η_0 values, and the subtraction prescription that corresponds to an $m_{1/2}$-dependent initial condition $\tilde{\eta}_0$. Of course, the absolute value of $V_{\rm full}$ depends very much now on the initial condition for η, but this is a constant shift as far as the Q dependence is concerned. Note that, strictly speaking, to ensure the RG invariance at one-loop level one should not consider the running of parameters within the one-loop expressions in (3.16) [42,48], since those induce formally two-loop order terms. Indeed, as we have checked explicitly, the scale independence of the full effective potential at one-loop is almost perfect when freezing the running of all relevant parameters entering the different one-loop contributions, while the formally higher-order terms induced from those runnings produce a remnant but rather moderate scale dependence visible in Fig. 1. We have checked

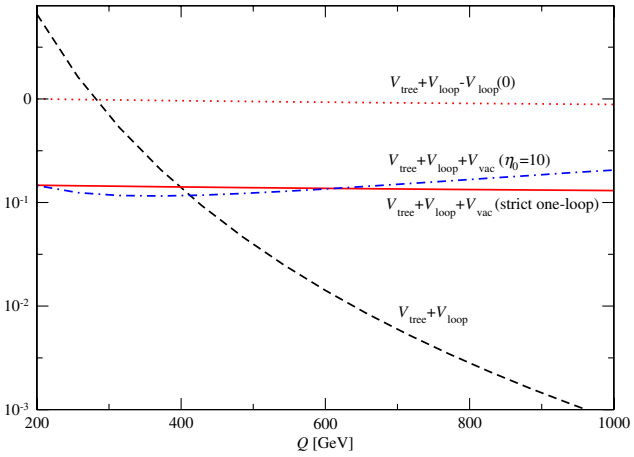

FIG. 1 (color online). The scale dependence of the effective potential, with or without the vacuum energy contributions, for representative input values $B_0 = 0.2 m_{1/2}$, $m_0 = A_0 = 0$, $m_{1/2} =$ 300 GeV, and $m_{\rm top} = 173$ GeV. Dashed line: without vacuum energy contribution; full line: $V_{\rm full}$ from Eq. (3.16) with running vacuum energy and $\eta_0 = 10$ at the strict one-loop order (i.e. no running of parameters inside one-loop expressions); dash-dotted line: same as the previous case but with all running parameters at one-loop, showing moderate spurious scale dependence to be cancelled by two-loop contributions; dotted line: same with subtracted vacuum contribution from Eq. (3.15).

however that such spurious effects remain reasonably small in all cases of our subsequent analysis. In particular, they influence only very moderately the location of $m_{1/2}$ minima, whenever those exist.

B. The fate of $m_{1/2}$ minima

Having a well-defined (one-loop) RG-invariant effective potential, Eq. (3.16), we will now examine in more detail the behavior of its different contributions with respect to $m_{1/2}$. By inspection of the RGE, it is possible to infer that, for generic boundary conditions with a linear dependence upon the soft breaking parameters as given in (2.15), all the resulting RG-evolved parameters at the EW scale, in the one-loop RG approximation, will have a similar linear behavior,

$$B_{\rm EW} = b m_{1/2}, \qquad m^2_{H_u} = u m^2_{1/2},$$
$$m^2_{H_d} = d m^2_{1/2}, \qquad A_i = a_i m_{1/2}. \tag{3.21}$$

The unspecified scale-dependent b, u, d, and a_i parameters in Eq. (3.21) have of course complicated expression in terms of the original ones in Eq. (2.15), but entirely determined numerically by the RGEs. Note, indeed, that the linear behavior in Eq. (3.21) is obtained even for the strict no-scale boundary conditions in (2.10) because an extra $m_{1/2}$ linear dependence is induced from the RGE of the gaugino mass parameters M_i.

Although the order of the three different minimizations in Eqs. (3.4) and (3.7) is in principle irrelevant, before examining the $m_{1/2}$ minimization it is much more convenient to sit first at the EW minima, which greatly simplifies the procedure. (This is also because we do not consider the full expression of the one-loop effective potential for any H_u, H_d field values, since it is equivalent and more convenient to put the tadpole contributions when the effective potential is evaluated at the EW minimum.) This is just the familiar way of expressing the EW minimization Eq. (3.4) as constraints to express $B_{\rm EW}$ and $\mu_{\rm EW}$ in terms of the other parameters:

$$B\mu = (\hat{m}^2_{H_u} + \hat{m}^2_{H_d} + 2\mu^2)\frac{\sin 2\beta}{2}, \tag{3.22}$$

$$\mu^2 = \frac{\hat{m}^2_{H_d} - \hat{m}^2_{H_u}\tan^2\beta}{\tan^2\beta - 1} - \frac{g^2 + g'^2}{4}v^2, \tag{3.23}$$

where $\tan\beta \equiv v_u/v_d$, $v^2 = v_u^2 + v_d^2$ in our conventions, and $\hat{m}^2_{H_i} \equiv m^2_{H_i} + \delta H_i$, where $\delta H_{u,d}$ denotes the corrections implied by one-loop tadpoles. The latter have the generic form

$$\delta H_i = \frac{1}{16\pi^2}\sum_n c_n (-1)^{2n} M_n^2 \left(\ln\frac{M_n^2}{Q^2} - 1\right), \tag{3.24}$$

where c_n are the different couplings to the respective Higgs fields H_u, H_d of all relevant particles in the sum over n. Notice that, for reasons that will become clear in Sec. IV C, we did not yet use in Eq. (3.23) the additional constraint that the Z mass should be reproduced at the EW minimum, i.e. the *extra* constraint:

$$\frac{g^2 + g'^2}{2}v^2 \equiv m_Z^2. \tag{3.25}$$

As discussed above, one expects the soft SUSY-breaking parameters $m^2_{H_i}$ and B in no-scale scenarios to be directly related to the single source of SUSY breaking, $m_{3/2}$ (or equivalently $m_{1/2}$). Concerning the supersymmetric μ parameter, as stated at the end of Sec. II, it may either be considered as an independent parameter or else related to $m_{1/2}$ at high scale. But, it is in both cases entirely determined, at the EW scale, via the constraints (3.23). From (3.22), (3.23), and (3.24), one obtains, after straightforward algebra, the effective potential at the EW minimum in the form,

$$V_{\rm full}^{\rm EW\,min} = -\frac{g^2 + g'^2}{8}v^4(1 - 2s_\beta^2)^2 - v^2(s_\beta^2\delta H_u + c_\beta^2\delta H_d) + V_{\rm loop} + \tilde{\Lambda}_{\rm vac}, \tag{3.26}$$

with $c_\beta \equiv \cos\beta$, $s_\beta \equiv \sin\beta$, and all terms have implicitly a scale dependence here omitted for simplicity of notation. Requiring further the constraint of correct physical Z mass (3.25), one obtains

$$V_{\rm full}^{\rm EW\,min}(m_Z\ \text{fixed}) = -\frac{m_Z^4}{2(g^2 + g'^2)}(1 - 2s_\beta^2)^2 - 2\frac{m_Z^2}{(g^2 + g'^2)}(c_\beta^2\delta H_u + s_\beta^2\delta H_d) + V_{\rm loop} + \tilde{\Lambda}_{\rm vac}, \tag{3.27}$$

which is formally different from (3.26), in particular, as far as the functional $m_{1/2}$ dependence is concerned. We will come back to this point in more detail in the next section. Note that this difference is strengthened by the fact that the dependence on m_{H_u}, m_{H_d} has disappeared from the tree-level term of (3.26): indeed, away from the EW minimum the (tree-level) potential in Eq. (3.1) depends on the five parameters v_u, v_d, m_1^2, m_2^2, $B\mu$ (let alone the two gauge couplings). Now B and μ can be eliminated upon use of the EW minimum constraints (3.22) and (3.23), but the very structure of (3.1) implies that, at the EW minimum, a third parameter disappears so that (3.26) in fact depends only on two independent parameters, that we may choose here for convenience to be v_u and v_d.

IV. LOOKING FOR MINIMA OF THE RG-INVARIANT EFFECTIVE POTENTIAL

In this section, and before entering a more phenomenological discussion, we examine generically the possible existence and fate of $V_{\rm full}(m_{1/2})$ minima for representative

input parameters. We will also specify for this purpose some important aspects of our minimization procedure.

A. B_0 input

We shall first consider an important feature concerning the choice of the input parameters. Most scenarios in no-scale models imply a fixed B_0 high-scale value, in particular, in the strict no-scale, $B_0 = 0$ as in Eq. (2.10), or in the string-inspired case (2.13). However, the by-now standard MSSM model-independent procedure is to determine $B_{\rm EW}$ together with $\mu_{\rm EW}$ from the REWSB minimization conditions (3.4), not caring usually for high-scale values of B_0. Even in a more phenomenological framework, it is of interest to perform the minimization rather with B_0 input, considering $\tan\beta$ as dynamically determined rather than an input. Essentially, one has to consider Eq. (3.22) as determining $\tan\beta$ from $B_{\rm EW}$ and the other relevant parameters at the EW scale. It turns out to be a rather nontrivial exercise to make such a consistent algorithm. Actually, the EW minimization condition (3.4) together with $\tan\beta(B)$ determination turns out to give a fourth-order equation for $\tan\beta$ (with not always real solutions), but this is a rather straightforward part of the derivation. More problematic is that the dynamical $\tan\beta$ value thus determined at the EW scale is a sensible parameter in all subsequent calculations, and, in particular, it drastically affects the influential top Yukawa coupling [due to the low-energy matching relations Eq. (3.9)], which in turn is driving strongly the RGE of the B parameter. Therefore, the algorithmically nontrivial feature is to get consistent values of B_0 and $\tan\beta$, matching both high- and low-energy boundary conditions, satisfying the REWSB constraints etc., because of the induced effects on the RGE. This has to be solved iteratively and a new algorithm was introduced in SuSpect for this purpose.

We illustrate in Fig. 2 the connection between B_0 and $\tan\beta$ for different representative values of $m_{1/2}$. As one can see, rather low $\tan\beta$ values are favored, especially for increasingly large B_0. Note that Fig. 2 illustrates only the $m_0 = 0$ case, but the influence of $m_0 \neq 0$ is not very drastic, only pushing the curves for a given $B_0 \neq 0$ to slightly smaller $\tan\beta$, in an almost parallel way. The obtained values of $\tan\beta$ are essentially located in the range 2–25 (increasing for decreasing B_0 and increasing m_0) for 100 GeV $\lesssim m_{1/2} \lesssim \mathcal{O}(1$ TeV). It is still possible to reach larger $\tan\beta$ values, but for very large $m_{1/2}$ and small $B_0 \sim 0$ values.

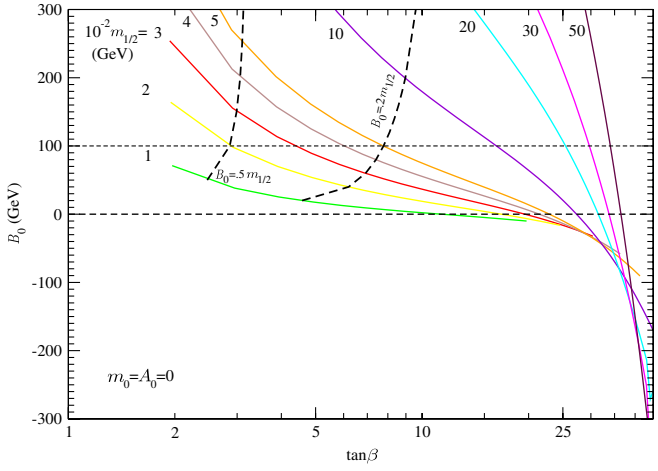

FIG. 2 (color online). The $B_0 - \tan\beta$ connection for various choices of $m_{1/2}$ (with $m_0 = A_0 = 0$).

B. Renormalization scale prescriptions and naive RG-improved effective potential

Since the full effective potential Eq. (3.16) is approximately scale independent (up to two-loop order), it is convenient to go a step further, following [21], and define a naive "RG-improved" effective potential by choosing the arbitrary scale Q_0 such that

$$V_{1-\rm loop}(Q_0) \equiv 0. \tag{4.1}$$

This choice simplifies largely the analysis since one can then consider only the minimization of $V_{\rm tree}(Q_0) + \tilde{\Lambda}_{\rm vac}(Q_0)$, which has a relatively simpler dependence on $m_{1/2}$. The latter combination still embeds one-loop corrections, since the dependence $Q_0(Q)$ at one-loop is implicit and thus consistently absorbed within $V_{\rm tree}(Q_0) + \tilde{\Lambda}_{\rm vac}(Q_0)$. This prescription is partly inspired by the construction of RG-improved effective potential [39–42], where RG-resummation properties have been rigorously established for simpler effective potentials with a single mass scale. In the present multiscale MSSM case, a rigorous generalization is not available at present, and choosing simply the scale cancelling the loop term is certainly not sufficient to establish correct resummation properties, but at least this prescription is well defined and greatly simplifies the analysis. An expression for Q_0 is obtained from Eqs. (3.10) and (3.11) in the form

$$Q_0 = e^{-3/4} \exp \frac{\sum_n (2s_n + 1) M_n^4(Q_0) \ln M_n^2(Q_0)}{2 \sum_n (2s_n + 1) M_n^4(Q_0)}, \tag{4.2}$$

which, at the one-loop level, gives explicitly Q_0. [The Q_0 dependence through $M_n(Q)$ on the RHS of Eq. (4.2) gives contributions formally of higher (two-loop) order. To include these effects, one can still solve (4.2) numerically by iterating on Q_0.] Nevertheless, the occurrence and location of possible no-scale $m_{1/2}$ minima are not expected to depend too much on this prescription, up to higher-order small effects, due to the overall approximate RG invariance. We emphasize that (4.2) is only one convenient choice among many possible prescriptions, and in our numerical analysis, as will be more explicit later, we also perform and compare the minimization results when using other well-defined renormalization scale prescriptions to

quantify the residual scale dependence. In those expressions is also implicit the field dependence of the masses: as mentioned above, minimizing with respect to the H_u, H_d field is more conveniently done by canceling the corresponding one-loop tadpoles [43], which is completely equivalent to minimizing explicitly with respect to the H_u, H_d fields.[5] All that is performed numerically within SuSpect [49], involving a number of subtleties like necessary iterations etc.

C. Different $m_{1/2}$ minimization procedures

Having determined the EW direction from Eq. (3.4), one obtains the effective potential (3.26) in the EW valley, $V_{\rm full}^{\rm EW\ val}(m_{1/2})$, and then performs the extra minimization Eq. (3.7) along this valley. In this subsection, we examine in some detail different approaches to this minimization procedure, having in mind what can be most easily implementable within the present tools for the computation of the MSSM spectra. Though we will carry out a numerical analysis with SuSpect at the full one-loop level (including dominant two-loop effects as well), it is useful at a first stage to examine some approximations to appreciate the main features of the minimization results.

At first sight, it could be very tempting to simply evaluate the full effective potential (3.16) from the output of one's preferred SUSY spectrum code, and to perform the extra minimization with respect to $m_{1/2}$ numerically. However, there is an important subtlety: in the no-scale approach, v_u, v_d, and $m_{1/2}$ should be treated as three independent dynamical variables with respect to which we seek a minimum of $V_{\rm full}$. It is only at such a minimum that one requires the physical quantities, such as the pole masses of the Z boson, the top and bottom quarks, the τ lepton (as well as the ones of all other quarks and leptons), to be properly reproduced. Now, the point is that in most publicly available SUSY spectra codes [49–52] only the v_u, v_d two-parameter EW minimization is performed. Accordingly, the m_Z, $m_{\rm top}^{\rm pole}$, and other mass constraints are hard-coded everywhere, which is perfectly consistent insofar as the EW minimization conditions (3.22) and (3.23) are by definition valid only at the minimum. In contrast, if one is determining possible $m_{1/2}$ minima through a numerical analysis of the shape of $V_{\rm full}^{\rm EW\ val}(m_{1/2})$, while requiring *beforehand* the above-mentioned mass constraints, which is the most straightforward way of using the existing codes, then this amounts to requiring the correct physical mass values even when not sitting at the physical vacuum. This induces an artificial dependence of the soft parameters on $m_{1/2}$ distorting the shape of $V_{\rm full}^{\rm EW\ val}(m_{1/2})$ and thus the location or even the possible existence of the minima. More specifically, assuming (2.15) for definiteness and fixing m_Z away from the $m_{1/2}$ minimum induces through (3.23) and (3.25) a functional dependence of μ on $m_{1/2}$, which is incompatible with an (otherwise perfectly acceptable) $m_{1/2}$-independent boundary condition for μ, or even with a boundary condition having an $m_{1/2}$ functional dependence of the type (2.16). Feeding back in (3.26) this fixed-m_Z induced $\mu(m_{1/2})$ would lead to an EW valley potential $V_{\rm full}^{\rm EW\ val}(m_{1/2})$ that is incompatible with a large class of possible boundary conditions for μ, and to the false conclusion that they are forbidden. In practice, this would show up in a modification of $\frac{\partial\mu}{\partial m_{1/2}}$ in the identity

$$\frac{d}{dm_{1/2}} V_{\rm full}^{\rm EW\ val}(m_{1/2}, \mu) = \frac{\partial}{\partial m_{1/2}} V_{\rm full}^{\rm EW\ val} + \frac{\partial V_{\rm full}^{\rm EW\ val}}{\partial \mu} \frac{\partial \mu}{\partial m_{1/2}}, \tag{4.3}$$

which would displace the solutions of $\frac{d}{dm_{1/2}} V_{\rm full}^{\rm EW\ val}(m_{1/2}, \mu) = 0$. A similar rationale holds for the physical value of $m_{\rm top}^{\rm pole}$ when fixed beforehand. In this case, Eq. (3.9) induces a spurious dependence of $Y_t(Q_{\rm in})$ on $m_{1/2}$ through v_u as well as the non-RGE loop corrections $\delta_y^{\rm RC}(Q_{\rm in})$. When fed back in the potential along the EW valley, such a dependence will again distort unphysically its shape.

In order to avoid all these difficulties, one can adopt three possible procedures:

(A) derive an explicit form for (3.7), akin to the explicit forms (3.22) and (3.23), derived from (3.3), and solve numerically this system of three explicit equations. This permits to use consistently the fixed mass constraints (as they stand in the public codes without modification), since one is now sitting at the actual physical vacuum.

(B) deactivate the physical mass constraints in the codes, determine numerically the minimum of $V_{\rm full}^{\rm EW\ val}(m_{1/2})$ along the EW valley, then impose these mass constraints once the minimum is found, to check for consistency.

Implementation of procedure (B) including the full-loop-level effective potential, can be very involved and would necessitate a highly nontrivial extension of the standard procedures of the various public codes. Although the EW minimization part would not change,[6] the further minimization with respect to $m_{1/2}$, (3.7), if performed purely numerically, becomes in general a rather involved task; in the EW valley, one will have to scan a two-parameter

[5]The equivalence only holds when sitting at the EW minimum, as the cancellation of the tadpoles does not give the field dependence *away* from the EW minimum.

[6]The explicit forms at the full one-loop level, (3.22) and (3.23), should still be solved numerically due to the tadpoles involving a highly nonlinear dependence on all parameters.

space $(m_{1/2}, \mu)$, requiring the correct $\mu(m_Z)$ relationship via (3.23), (3.25), as well as consistency of $m_{\rm top}^{\rm pole}$ via (3.9), only once the minimum is found. This holds irrespective of whether we assume (2.16) or not. However, as we will discuss below, the boundary condition (2.16) will have the benefit that requiring the mass constraints *before* determining the minimum, although in principle wrong, can become a good approximation. This allows a simplified version of (B) as follows:

(C) in this procedure, the minimum of $V_{\rm full}^{\rm EW\ val}(m_{1/2})$ is determined fully numerically along the EW valley as in (B), but the m_Z and $m_{\rm top}^{\rm pole}$ constraints are applied from the outset as in (A).

Procedure (C) is thus desirable as it provides a simpler picture and is easy to use, not needing drastic modification of the present codes. The boundary condition (2.16) has also some practical benefits in the context of procedure (A), as it allows to obtain an explicit analytical form for (3.7), which otherwise would not be easily tractable if μ were taken as a free parameter. In the sequel, we will thus stick to (2.16) in all our study when comparing the outcome of procedures (A) and (C). Furthermore, as a consequence of the RGE of μ, which is of the form $d\mu/d\ln Q \sim \mu$, the boundary condition assumption (2.16) leads to

$$\mu(Q) = c_\mu(Q) m_{1/2} \tag{4.4}$$

that is valid at any scale Q. Now, since $\mu_{\rm EW} \equiv \mu(Q_{\rm EW}^{\rm default})$ is anyway fixed *a posteriori* by the EW minimization and the m_Z constraint, Eqs. (3.23) and (3.25), its high-scale value μ_0 is entirely determined through the RGE from $\mu_{\rm EW}$. Yet, one has still to verify that μ_0 remains of order $m_{1/2}$ in the spirit of the no-scale framework, as emphasized at the end of Sec. II. Indeed, this is generically the case (except possibly for $\tan\beta$ very close to 1, which is anyway phenomenologically largely excluded), given the structure of (3.23) and the fact that $\mu(Q)$ does not run much.

We now discuss in more detail the implementation of procedures (A) and (C) as well as the approximate validity of the latter. Using (2.15) and (2.16) and neglecting the running of all masses occurring in the one-loop part of (3.16), which is consistent at one-loop level strictly, one can derive from (3.16) an "explicit" equation for (3.7) to be used in procedure (A):

$$\begin{aligned} & m_{1/2}\frac{\partial}{\partial m_{1/2}} V_{\rm full}(m_{1/2}) = 0 \\ & \Rightarrow V_{\rm full}(m_{1/2}) + \frac{1}{128\pi^2}\sum_n (-1)^{2n} M_n^4(m_{1/2}) \\ & \quad + \frac{1}{4} m_{1/2}^5 \frac{d\tilde{\eta}_0}{dm_{1/2}} = 0, \end{aligned} \tag{4.5}$$

where we also used (3.20). Various comments are in order concerning the validity of this equation. The assumptions (3.21) and (2.16) are crucial to derive this compact expression, since the first term $V_{\rm full}$ on the RHS of (4.5) originates (upon use of $m_{1/2}\partial_{m_{1/2}}(m_{1/2}^4) = 4m_{1/2}^4$) from all terms within $V_{\rm full}$ that scale trivially as $m_{1/2}^4$, while the supertrace term comes from the explicit $\ln(m_{1/2}^2/Q^2)$ dependence within (3.11), see e.g. Refs. [27–29]. There is, however, more to it. Since the squared-mass eigenvalues M_n^2 in (3.10) are H_u-, H_d-field dependent, then strictly speaking the scaling $M_n^2 \sim m_{1/2}^2$ assumed in deriving (4.5) does not hold in general. There should thus be extra terms in (4.5) due to the breakdown of the $m_{1/2}$ scaling. Such terms are indeed present in general, but they actually vanish when the conditions (3.3) are taken into account, i.e. at the true electroweak vacuum.[7] Obviously, such a scaling holds as well at the point $H_u = H_d = 0$, in particular, for the RGE of $\tilde{\Lambda}_{\rm vac}$, (3.17). It then immediately follows from (3.20), (3.21), and (4.4) that the running of $\tilde{\eta}$ does not depend on $m_{1/2}$. Thus, the only possible dependence of $\tilde{\eta}$ on this parameter would come from the boundary condition, whence the last term on the RHS of (4.5). This term, usually not considered in the literature, will be important when discussing the alternative subtraction prescription in Sec. IV E. At this point, Eqs. (3.22), (3.23), and (4.5) form a consistent set of REWSB conditions given the assumptions (2.15) and (2.16). In a more general context, one would still want to consider models where the (supersymmetric) parameter μ_0 is an independent one at high scale so that the scaling (2.16) does not hold, (reflecting the well-known μ-parameter problem). In this case, Eq. (4.5) will have to be modified in a nontrivial way including additional terms involving essentially $\partial V_{\rm full}/\partial\mu$ that are not straightforward to evaluate for $V_{\rm loop}$.[8]

Equation (4.5), together with (3.22) and (3.23), completes the ingredients of procedure (A). They will have to be solved numerically as a nontrivial system of equations giving the values of $m_{1/2}$, v_u, and v_d at the minimum of the potential.

We turn now to procedure (C) and discuss the degree of validity of the approximation involved when m_Z is fixed before minimization. To illustrate the case, we focus first on the tree-level part of the potential (3.26). Before fixing m_Z, there is evidently a nontrivial $m_{1/2}$ dependence in this part, in the EW valley; from Eqs. (3.22) and (3.23), v_u and v_d (or v and s_β^2) can be reexpressed in terms of the soft parameters and μ as

[7]This is not specific to our boundary condition assumptions. For any function $V(\chi, \phi)$ with χ and ϕ two independent fields, one can always artificially treat ϕ as being linear in χ, $\phi \equiv \chi\hat{\phi}$, to recast $\partial_\chi V(\chi, \phi)$ in the form of a *total* derivative $\frac{d}{d\chi}V(\chi, \chi\hat{\phi})$, provided one considers only the points where $\partial_\chi V(\chi, \phi) = \partial_\phi V(\chi, \phi) = 0$.

[8]The exploration of this more general case will be pursued elsewhere.

$$v^2 = -\frac{2}{(g^2+g'^2)}\left(\frac{m_{H_u}^2 - m_{H_d}^2}{|\cos 2\beta|} + m_A^2\right), \tag{4.6}$$

with

$$|\cos 2\beta| = \left(1 - 4\frac{B^2\mu^2}{m_A^4}\right)^{1/2}, \tag{4.7}$$

where we defined for convenience $m_A^2 \equiv m_{H_u}^2 + m_{H_d}^2 + 2\mu^2$, so that

$$V_{\text{tree,EW min}} = -\frac{1}{2(g^2+g'^2)}(m_{H_d}^2 - m_{H_u}^2 - m_A^2|\cos 2\beta|)^2, \tag{4.8}$$

which therefore exhibits an explicit nontrivial $m_{1/2}$ dependence via the relations in (3.21). Thus, one easily infers that $V_{\text{tree,EW min}} \sim m_{1/2}^4$. In contrast, if one imposes first m_Z via Eq. (3.25) (as is hard-coded in the public version of SuSpect and in other public codes [50–52]), clearly the effective potential has then a different $m_{1/2}$ dependence as is explicit from (3.27), whose tree-level part only depends on m_Z and $\tan\beta$: it has accordingly practically no more dependence on $m_{1/2}$ (at least a very mild one as compared to the $m_{1/2}^4$ dependence inferred from the previous analysis not fixing m_Z). This illustrates the point we stressed previously in this section: fixing m_Z via Eq. (3.23) beforehand induces a spurious functional dependence, $\mu \equiv \mu(m_{1/2}, m_Z)$, which overwrites any initial assumption about the μ boundary condition and thus modifies unphysically the structure of the minima. This remains of course true beyond the tree level. More generally, it is clear from (4.3) that the reliability of procedure (C) will depend on how far or close is the spurious dependence $\mu(m_{1/2}, m_Z)$ from the initially assumed model-dependence $\mu(m_{1/2})$. For instance, if μ is taken to be a free $m_{1/2}$-independent parameter, then obviously the second term on the RHS of (4.3) should be vanishing, while within procedure (C) this is not the case and can even lead to substantial differences for large $m_{1/2}$, thus degrading the quality of the approximation in determining the actual minimum. In contrast, the situation is much more favorable when the boundary condition (2.16) is assumed. As can be easily seen from (3.23), (3.21), and (3.25), the spurious dependence is of the form $\mu(m_{1/2}, m_Z) = (\frac{u\tan^2\beta - d}{1-\tan^2\beta} m_{1/2}^2 - \frac{m_Z^2}{2})^{1/2} \sim m_{1/2}$ in the limit $m_{1/2} \gg m_Z$, and the functional dependence in (4.4) is properly reproduced at the electroweak scale in this limit. Moreover, relatively large $m_{1/2}$ values are favored by the most recent experimental exclusion limits. From this rather crude analysis, it is expected that as far as the effect of fixing m_Z is concerned, the (relative) difference between the output of procedures (A) and (C) should decrease like $\sim m_Z^2/m_{1/2}^2$ for increasing $m_{1/2}$. We have performed explicit minimizations for rather generic mSUGRA input with $B_0, m_0, \cdots \neq 0$ to compare both procedures, and checked that the above-described qualitative behavior is indeed essentially observed. The corresponding $m_{1/2}$ minima that can be obtained from the naive (incorrect) procedure can differ substantially for $m_{1/2} \sim m_Z$, while for $m_{1/2} \gtrsim 300$ GeV the difference between the two procedures decreases to reach about 10% for larger $m_{1/2}$, as will be illustrated with concrete examples. The residual 10% difference is not due to the fixing of m_Z but actually essentially to the effect of fixing $m_{\text{top}}^{\text{pole}}$ through (3.9), which was not taken into account in the above discussion. It is, furthermore, always positive in a large part of the parameter space. More precisely, the leading non-RGE one-loop SUSY corrections in (3.9) have the generic form

$$\delta_{\text{SUSY}}^{\text{QCD}} = \frac{\alpha_s}{3\pi}\left(r + 2\ln\frac{m_{1/2}}{m_Z}\right), \tag{4.9}$$

where we used (3.21) and (4.4) and where r is a complicated function of b_0, x_0, a_0 of order 1–2 depending on the input values. The $\ln\frac{m_{1/2}}{m_Z}$ dependence translates through the induced $m_{1/2}$ dependence in Y_t into a shift of the form $\zeta m_{1/2}^4$ in (4.5), which *in fine* accounts for the above-mentioned constant relative difference in the values of $m_{1/2}$ minima.

With these features in mind, we will illustrate in most of our subsequent numerical analysis the results of both procedures (A) and (C).

D. No-scale scenarios and vacuum energy

We now illustrate minimization results for a representative set of parameter values, adopting the previously described prescriptions and minimization procedures, as well as the following three different choices of EW scale:

(1) the "default" scale,

$$Q_{\text{EW}}^{\text{default}} = (m_{\tilde{t}_1} m_{\tilde{t}_2})^{1/2}, \tag{4.10}$$

largely adopted in nowadays SUSY spectrum calculations.

(2) the scale Q_{EW} such that

$$V_{1-\text{loop}}(Q_{\text{EW}}) = 0, \tag{4.11}$$

as motivated previously in Sec. IV B, so that the expression being minimized is $V_{\text{tree}} + \tilde{\Lambda}_{\text{vac}}$. This scale is to be determined dynamically according to Eq. (4.2).

(3) the scale Q_{EW} such that

$$\tilde{\Lambda}_{\text{vac}}(Q_{\text{EW}}) = 0, \tag{4.12}$$

TABLE I. Values of $m_{1/2}$ minima and the corresponding values of $Q_{\rm EW}(m_{1/2})$, for $m_0 = A_0 = 0$, $B_0 = 0.2m_{1/2}$, $\eta_0 = 10$, and three different scales, using the two minimization procedures (A) and (C). A conservative intrinsic numerical error of about 1% is to be added, taking into account uncertainties in the RGE and spectrum calculations. We also indicate for comparison the value of Q at the EW border of (3.5).

	$Q_{\rm EW} = (m_{\tilde{t}_1} m_{\tilde{t}_2})^{1/2}$	$V_{1-\rm loop}(Q_{\rm EW}) = 0$	$\Lambda_{\rm vac}(Q_{\rm EW}) = 0$	EW border
1) procedure (A):				
$Q_{\rm EW}$ (GeV)	610	307	500	700
$m_{1/2}$ (min) (GeV)	335	332	334	⋯
$\eta_{\rm EW}$	1.1	−0.6	0	
2) procedure (C):				
$Q_{\rm EW}$ (GeV)	544	277	430	580
$m_{1/2}$ (min) (GeV)	297	299	300	⋯
$\eta_{\rm EW}$	0.6	−1.15	0	

motivated by the requirement of a vanishingly small vacuum energy at the EW scale.[9] Eq. (4.12) has also to be solved iteratively, since a different choice of $Q_{\rm EW}$ affects the whole spectrum.

As it turns out, these three scales are all quite different numerically, so that the comparison of the ensuing results is expected to be a reasonably good cross-check of the (necessarily approximate) scale invariance of our minimization results. Note moreover that the three choices correspond to dynamically determined scales, being all nontrivial functions of $m_{1/2}$ rather than fixed values.

In Table I, we summarize, for $m_0 = A_0 = 0$, $B_0 = 0.2m_{1/2}$, and $\eta_0 = 10$, the resulting $m_{1/2}$ minima and the corresponding values of the $Q_{\rm EW}$ scale for these three scale prescriptions, using both the (A) and (C) procedures described in Sec. IV C. A first welcome feature is that the existence and values of the minima do not depend much on the choice of scale, at one-loop order, as expected if RG invariance is consistently implemented. We have checked that the same rather generic properties are observed for other values of the input parameters. (We comment more on those checks later in this section.) Another feature is that there is a definite, but rather moderate, difference between the results of the two minimization procedures, procedure (A) giving generically slightly higher values of $m_{1/2}$ than procedure (C) (by about 10% here for $m_{1/2} \sim 300$ GeV). This confirms the discussion at the end of the previous section where the origin of this difference was traced back to the effect of fixing the physical top-quark mass prior to minimization in procedure (C).

But, perhaps the most important feature is that there exists a somewhat narrow window for $\eta(Q_{\rm EW})$ where the vacuum energy contribution is neither too large nor too small, compensating efficiently the behavior of the tree-level and loop contributions such as to produce nontrivial $m_{1/2}$ minima. For each value of η_0, the precise values of these upper and lower critical values of $\eta_{\rm EW}$ depend on B_0 (mildly) and on m_0, and also on the choice of renormalization/EW scale. For example, the case illustrated in Table I leads approximately to

$$-1.5 \lesssim \eta(Q_{\rm EW}) \lesssim 1.2, \tag{4.13}$$

with the GUT boundary condition $\eta_0 = 10$. Specific values of $\eta(Q_{\rm EW})$ within this range, corresponding to different $Q_{\rm EW}$ scales, are given in the table. In fact, the lower and upper bounds in (4.13) can be, respectively, associated to the lowest and highest values of $Q_{\rm EW}$ consistent with REWSB. For instance, $\eta \gtrsim 1.2$ could still lead to a minimum of the potential in the $m_{1/2}$ direction, but would require $Q_{\rm EW} > 580$ GeV, which is beyond the EW border (see Table I) so that there is no minimum in the v_u, v_d direction. As for the lower bound $\simeq -1.5$, although related to the same physical feature, its value is simply dictated by the lower bound $Q_{\rm EW} \gtrsim \mathcal{O}(m_Z)$, which is a natural requirement. We stress that, although corresponding to the same value of η_0 at the GUT scale, the various $\eta(Q_{\rm EW})$ in the range (4.13) do not lie on one and the same trajectory of the running $\eta(Q)$. The reason is as follows: when the REWSB is fulfilled, the values of $Y_t(Q_{\rm EW})$, determined from (3.9) with the physical $m_{\rm top}^{\rm pole}$ imposed, amount to different and incompatible boundary conditions for Y_t when varying the $Q_{\rm EW}$ prescription. This leads to a modification of the

[9]Note that this prescription is just a convenient choice. It is by no means intended as a cheap solution to the notorious "cosmological constant problem". For one thing, at the electroweak scale the true vacuum energy is not given by Λ, but by the value of $V_{\rm full}$ at the minimum, which has various tree-level and loop contributions for nonvanishing v_u, v_d and $m_{1/2}$. Then one could rather consider a scale prescription such as $V_{\rm full}(Q) = 0$. But again this is nothing but adjusting the minimum, requiring possibly a proper choice of the boundary condition $\Lambda^0 = \Lambda(Q_{\rm GUT})$, and certainly not more a solution to the "cosmological constant problem." More generally, the presently measured (small and positive) cosmological constant is a very large distance observable, and its relation to the very short distance vacuum energy computed from a well-defined quantum field theory is another side of the unsolved problem.

running of the MSSM parameters, in particular $m^2_{H_u}(Q)$, and so to a modification of the values taken by the beta function in (3.17) implying different running $\eta(Q)$ trajectories for different $Q_{\rm EW}$ prescriptions.

This point is important to keep in mind when discussing how allowed ranges for $\eta(Q_{\rm EW})$ such as (4.13) are mapped on allowed ranges of η_0 at the GUT scale. We illustrate in Fig. 3 the connection between low- and high-energy η values as dictated by the RG evolution supplemented with the $m^{\rm pole}_{\rm top}$ constraint, but now for a unique EW scale prescription $Q^{\rm default}_{\rm EW}(m_{1/2})$ given by (4.10). In this case, the induced difference in the boundary conditions for Y_t comes from the different values of $m_{1/2}$ minima. Thus, each full-line curve in the figure corresponds simultaneously to a different η_0, a different $m_{1/2}$ minimum, and different numerical values for the beta function in (3.17). It is then clear why, in contrary to what (3.17) would naively dictate, these curves are not globally shifted with respect to each other and can even intersect. Moreover, there is in general no simple one-to-one correspondence between the low-energy and high-energy values of η when the physical REWSB constraints are taken into account, since varying the $Q_{\rm EW}$ prescription would result in a beam of trajectories for each value of η_0, which can overlap at low Q. It follows that the lower and upper bounds on η_0 are somewhat tricky to determine precisely, as they correspond to an envelope deduced from the largest allowed range for $\eta(Q_{\rm EW})$ at the EW scale. Hereafter, we only give a qualitative discussion. An approximate range of η_0, for which $m_{1/2}$ minima exist, is given by

$$0 \lesssim \eta_0(Q_{\rm GUT}) \lesssim 15, \tag{4.14}$$

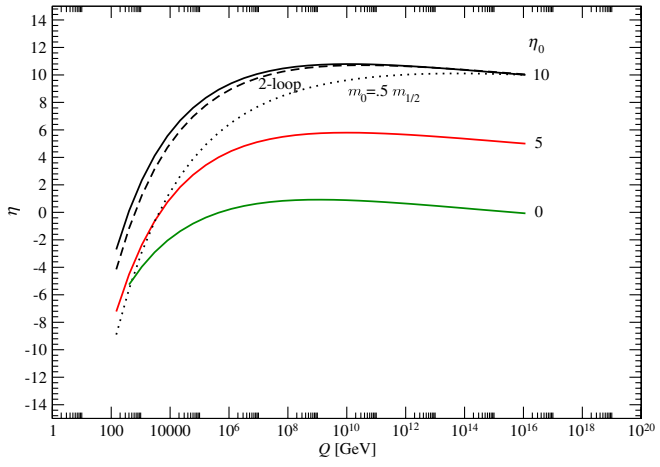

FIG. 3 (color online). The one-loop RG evolution of the vacuum energy between the EW and GUT scales, for $m_0 = A_0 = 0$, $B_0 = 0.2m_{1/2}$, $Q_{\rm EW} = (m_{\tilde t_1} m_{\tilde t_2})^{1/2}$, and three different sets of $(\eta_{\rm EW}, m_{1/2})$ as determined by the minimum of the potential; the corresponding η_0 values at the GUT scale are explicitly indicated. For $\eta_0 = 10$, we also show the RG evolution including two-loop effects (dashed line) and the $m_0 = 0.5m_{1/2}$ case (dotted line), for comparison. See text for further comments.

and the corresponding largest allowed range at the EW scale is found to be

$$-3 \lesssim \eta(Q_{\rm EW}) \lesssim 1.7. \tag{4.15}$$

Actually, this EW range is obtained from the beam of RG trajectories of $\eta_0 = 15$ alone, when spanning all possible $Q_{\rm EW}$ choices. It encompasses all other ranges corresponding to lower η_0 values. Figure 3 is also instructive as regards the connection between η_0 and $m_{1/2}$, given that whatever the precise choice of $Q_{\rm EW}$ prescription the latter remains of the same order of magnitude as $m_{1/2}$. Accordingly, the location of the $m_{1/2}$ minimum is quite sensitive to η_0, as illustrated in Table II for three representative values of η_0. In (4.14), the largest $10 \lesssim \eta_0 \lesssim 15$ values correspond to $m_{1/2} \lesssim 330$ GeV approximately. Though it will depend on the precise values of the other input parameters B_0 and m_0, one may anticipate that $\eta_0 \gtrsim 10$ is at the verge of being excluded in a substantial part of the other mSUGRA parameter space by present collider (CERN LEP, Tevatron and LHC) constraints, as we shall investigate in more detail in Sec. V. On the lower side of the η_0 range, $\eta_0 \lesssim 3$ in (4.14) corresponds already to $m_{1/2}(\min) \gtrsim 4$ TeV, and $m_{1/2}(\min)$ increases very rapidly to extremely large $m_{1/2}(\gg 1$ TeV) for lower values of η_0.

This behavior is rather generic and not very strongly dependent on B_0. Varying m_0 has a more substantial effect as illustrated on Fig. 3: for a given η_0, increasing the ratio $m_0/m_{1/2}$ will result in larger values of possible $m_{1/2}$ minima. Including two-loop RGE effects for the vacuum energy induces some systematic large shifts of about 20% of the $m_{1/2}$ minima found in Table I, but the results remain qualitatively similar. Pushing it to an extreme, one can extrapolate this behavior down to $\eta_0 \simeq 0$, which would lead to $m_{1/2}$ minima of order 50–80 TeV, corresponding, respectively, to large ($\simeq 50$) and small ($\simeq 10$) $\tan\beta$ values. All sparticles have then tens of TeV masses while the lightest Higgs mass remains of order 135 GeV, a not-very-exciting scenario for SUSY searches at the LHC.[10] We also observe that the sensitivity to the different scale choices tends to increase as η_0 decreases ($m_{1/2}$ increases); in other words, the precise determination of $m_{1/2}(\min)$ somewhat degrades, reflecting the increasing influence of ignored higher-order terms.

In Table II, we also give, for each $m_{1/2}$ minimum that we found, the corresponding range of values for $\tan\beta$ and for some of the most relevant sparticle masses, when different scale prescriptions are applied. We indicate as well the corresponding values of c^0_μ, cf. Equation (2.16); the latter is entirely determined by the RGE and the EW constraints (3.23) and (3.25) and comes out of order 1, as expected from the discussion following (4.4).

[10]It is amusing to note here that such a configuration, with an obviously severe electroweak fine-tuning problem, comes along with a vanishing vacuum energy at the GUT scale.

TABLE II. $m_{1/2}$ minima values for the two minimization procedures and different η_0, with corresponding values of $\tan\beta$. Other input are $B_0 = 0.2m_{3/2}$, $m_0 = A_0 = 0$. The variation of $m_{1/2}$ minima values corresponds to the various renormalization/EW scales, similarly to Table I. We also give some of the phenomenologically most relevant sparticle masses ($m_{\tilde{q}\,\mathrm{min}}$ designates the lightest squark of the first two generations).

Minimization procedure	η_0	$m_{1/2}$ (min)	$\tan\beta$ (Q_{EW})	c^0_μ	m_h	$m_{\chi^0_1}$	$m_{\tilde{\tau}}$	$m_{\tilde{q}\,\mathrm{min}}$	$m_{\tilde{g}}$
(A)	10	332–335	6.9–7.1	~0.82	~111	132–133	125–126	692–698	785–791
(C)	10	297–300	6.9–7.1	~0.8	~110	117–118	112–114	626–632	708–715
(A)	8	550–570	7.7–7.9	~0.86	~115	227–235	202–209	1093–1129	1250–1293
(C)	8	490–505	7.7–7.9	~0.85	~114	200–207	180–185	984–1012	1124–1156
(A)	5	1540–1560	9.5–9.7	~0.99	~121	670–679	552–559	2789–2822	3240–3288
(C)	5	1340–1360	9.5–9.7	~0.97	~121	579–588	481–488	2457–2490	2854–2894

An important consequence of the analysis is that the contribution of $\tilde{\Lambda}_{\mathrm{vac}}$ to the vacuum energy, necessary to define an RG-invariant effective potential making it an inseparable part of V_{full}, plays also a crucial role in the occurrence of the $m_{1/2}$ minima. In the early studies of no-scale minima [21] (where this contribution was not included), the parameter choices were mostly such that $m_{1/2}(m_{3/2})$ minima were of order m_Z, so that these minima resulted from a fair balance of tree-level and one-loop terms in the effective potential. But, given the present phenomenological constraints on $m_{1/2}$ and the behavior of the tree and loop contributions (including a much heavier top-quark mass than assumed in the early days) the situation has now notably changed. For instance, using the scale prescription (4.10), one finds that for larger $m_{1/2}$, say $m_{1/2} \gtrsim 300$ GeV (largely favored by the latest LHC results), the occurrence of these minima is essentially driven by the balance between $\tilde{\Lambda}_{\mathrm{vac}}$ and loop contributions. The latter have a clear $\sim m^4_{1/2}$ behavior, while the tree-level contributions tend to be relatively suppressed for large $m_{1/2}$; see Fig. 4(a) for an illustration of this case. However, one should keep in mind that a comparison of the relative tree-level versus loop-level and/or vacuum energy contributions does not make much sense physically since they are not separately RG invariant. Varying the scale Q shifts parts of $V_{1-\mathrm{loop}}$ into V_{tree} or $\tilde{\Lambda}_{\mathrm{vac}}$ and vice versa. It is even possible to choose the renormalization/EW scale $Q_{\mathrm{EW}} = Q_0(m_{1/2})$ such that one of these contributions, or some combination of them, vanishes identically for arbitrary $m_{1/2}$. In the example illustrated in Fig. 4(b), all of $V_{1-\mathrm{loop}}$ is absorbed in $\tilde{\Lambda}_{\mathrm{vac}}$ and tree-level contributions modifying consistently their individual shapes in $m_{1/2}$. However, once combined, they lead to essentially the same value of $m_{1/2}$ at the minimum irrespective of the scale prescription, as expected from the RG invariance of V_{full} and $dV_{\mathrm{full}}/dm_{1/2}$. Comparing Figs. 4(a) and 4(b) shows indeed a sufficiently good numerical stability of V_{full} and of the value of $m_{1/2}$ at its minimum, against a variation of the renormalization/EW scale.

The dominance of the loop and vacuum contributions with respect to the "tree-level" ones, as manifest for instance in Fig. 4(a) for large $m_{1/2}$ and the choice (4.10)

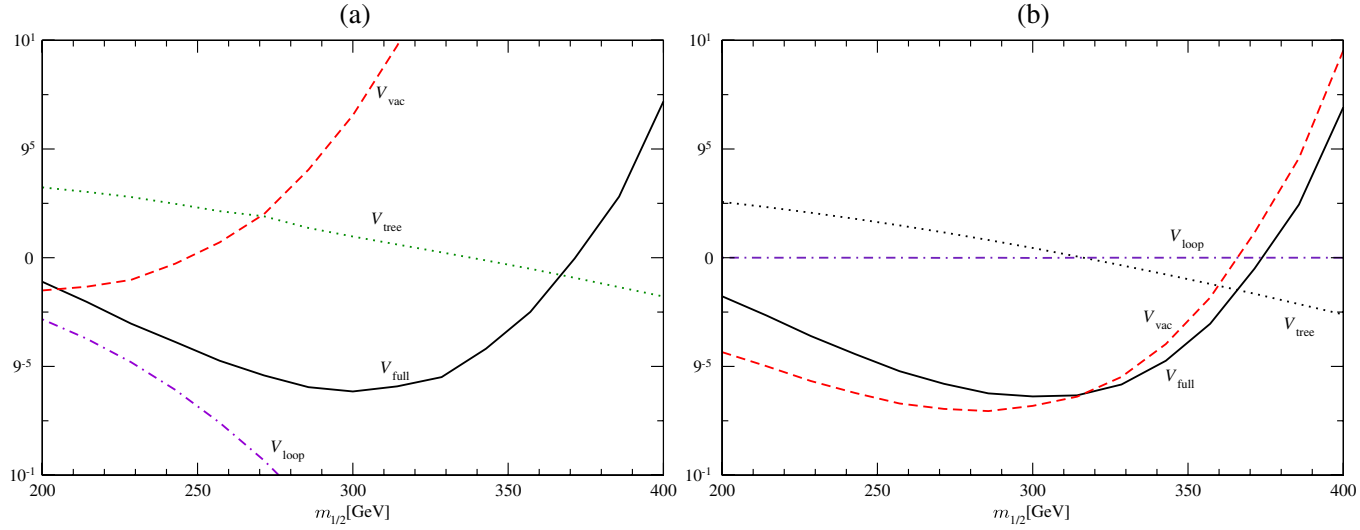

FIG. 4 (color online). Relative contributions of V_{tree}, $\tilde{\Lambda}_{\mathrm{vac}}$, and V_{loop} to V_{full} as functions of $m_{1/2}$ (for $m_0 = A_0 = 0$), for two different choices of the renormalization/EW scale, using (4.10) in (a), and (4.11) in (b).

for the EW scale, should not by itself question the validity of the perturbative expansion. For one thing, (4.10) is supposed to partly resum the dominant higher-order leading logs, and is thus in some sense safe (notwithstanding the multimass scale difficulties mentioned in Sec. IV B). For another, the one-loop and vacuum energy relative contributions are further enhanced due to a large cancellation in the tree-level contribution (especially for sufficiently large $\tan\beta$), which makes the latter a very shallow function of $m_{1/2}$ for a large class of $Q_{\rm EW}$ prescriptions. In that sense, it is not so much a problem of uncontrolled higher perturbative orders, but a rather accidental very mild dependence of the tree level on the relevant minimization parameter.

Finally, the two-loop contributions to the effective potential, though certainly non-negligible in practice, are known to remain well under control [45,46] for the rather moderate values of $m_{1/2} \lesssim 1$ TeV that are most phenomenologically interesting, and the perturbative validity is not endangered. We have included their dominant $\mathcal{O}(\alpha_s Y_t^2)$ contributions [45,53] and found that they stay at a reasonable level so that the resulting minima are rather stable. For very large values of $m_{1/2}$ well beyond the TeV range, there may be a true perturbativity problem, so that one may not trust too much the $m_{1/2}$ minimization results.

E. Alternative subtraction prescription

We have also analyzed for completeness the structure of the $m_{1/2}$ minima when adopting the subtraction prescription (3.15) rather than the untwiddled η prescription. In this section, we compare the outcome of the two prescriptions for a representative set of boundary values for B_0, m_0, and A_0. For the subtraction prescription, Eq. (4.5) can be recast in the more convenient form,

$$V_{\rm full}(m_{1/2}) + \frac{1}{128\pi^2}\sum_n (-1)^{2n}[M_n^4(m_{1/2}) - M_n^4(m_{1/2}, v_u = v_d = 0)] = 0. \quad (4.16)$$

Since this prescription provides a special case of the $m_{1/2}$-dependent $\tilde{\eta}_0$ boundary conditions, viz. (3.18) and (3.19), one expects it to lead to a different shape of $V_{\rm full}(m_{1/2})$ than the untwiddled η prescription, i.e. not just a constant shift, but rather a different structure of the minima in the $m_{1/2}$ direction. For the same reason, the comparison between the minimization procedures (A) and (C) of Sec. IV C, carried out in Sec. IV D for the untwiddled η prescription, does not necessarily hold for the subtraction prescription. In particular, as we will see, the very existence of $m_{1/2}$ minima may now not be necessarily guaranteed simultaneously in both procedures (A) and (C), in contrast to what was found in Sec. IV D. We show in Fig. 5 the various dependencies of $\tilde{\eta}$ on $m_{1/2}$ taken *at the electroweak scale* with Q fixed to $Q_{\rm EW}^{\rm default}$ as defined by (4.10) and boundary conditions $m_0 = A_0 = 0$, $B_0 = 0.2 m_{1/2}$. Following our previously defined conventional notations, $\tilde{\eta}$ represents here either $-V_{\rm sub}/m_{1/2}^4$ or the (untwiddled) η. In order to understand better the meaning of this plot, we stress that the $m_{1/2}$ dependence in $\tilde{\eta}$ has three different sources—the boundary condition $\tilde{\eta}_0$, the EW scale $Q_{\rm EW}^{\rm default}(m_{1/2})$, and the fixing of m_Z and $m_{\rm top}^{\rm pole}$ leading to $\mu_{\rm EW}(m_{1/2})$ and $Y_{\rm top}(m_{1/2})$. The two full-line curves indicated as "critical minima" on Fig. 5 are actually the locations of the $m_{1/2}$ minima as determined by procedure (A), that is where Eq. (4.5) is satisfied; the (red) upper full-line curve corresponds to $\tilde{\eta} \equiv -V_{\rm sub}/m_{1/2}^4$ and the (black) lower full-line curve to $\tilde{\eta} \equiv \eta$, taken at the electroweak scale.[11] The outcome of procedure (C) is always below those critical curves, due to the shift to lower $m_{1/2}$ minima by about 10% induced mainly by the fixing of $m_{\rm top}^{\rm pole}$, as discussed at the end of Sec. IV C and in Sec. IV D, Tables I and II. It is then easy to trace the structure and existence of $m_{1/2}$ minima by overlaying various curves of $-V_{\rm sub}/m_{1/2}^4$ and η, corresponding to different boundary

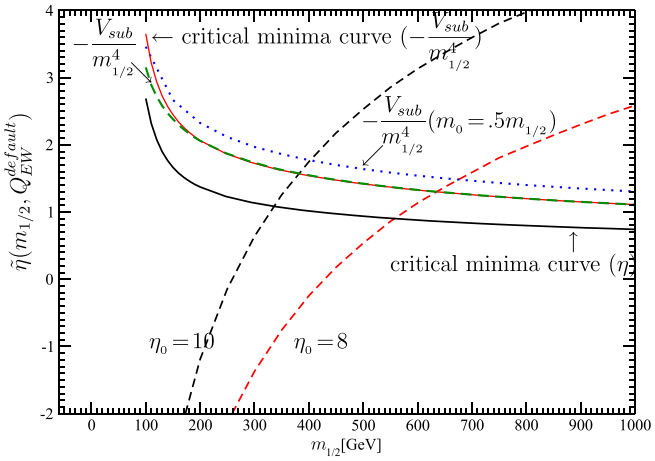

FIG. 5 (color online). The $m_{1/2}$–$\tilde{\eta}(Q_{\rm EW}^{\rm default})$ correlations. All curves (apart from the [blue] dotted curve) correspond to $m_0 = A_0 = 0$ and $B_0 = 0.2 m_{1/2}$ and $Q_{\rm EW}^{\rm default} \equiv (m_{\tilde{t}_1} m_{\tilde{t}_2})^{1/2}$. The two critical minima full-line curves give the locations of the $m_{1/2}$ minima for a given $\tilde{\eta}(Q_{\rm EW}^{\rm default})$ as determined by procedure (A), Eq. (4.5). (The [red] upper curve corresponds to $\tilde{\eta} \equiv -V_{\rm sub}/m_{1/2}^4$ and the [black] lower curve to $\tilde{\eta} \equiv \eta$.) The dashed-line curves give $\eta(m_{1/2}, Q = Q_{\rm EW}^{\rm default})$ for different boundary η_0, as induced by the RGE. Similarly, the (green) dashed-line curve almost coinciding with the critical full-line corresponds to the subtraction prescription.

[11] Each of these two cases satisfies (4.5), where, as emphasized previously, the latter equation has been derived before imposing the physical mass constraints. This is encoded in the fact that $d\tilde{\eta}_0/dm_{1/2}$ appears in (4.5), rather than $d\tilde{\eta}/dm_{1/2}$, so that this term is nonvanishing for $\tilde{\eta} \equiv -V_{\rm sub}/m_{1/2}^4$ but vanishes for $\tilde{\eta} \equiv \eta$. This is not in contradiction with the fact that $\tilde{\eta}$ has in both cases a nontrivial dependence on $m_{1/2}$ but only at the electroweak scale, as visible on the plot.

values of η_0 and (2.15), and looking for intersections with the two critical curves. For instance, the intersections between the η critical curve and the set of curves with different $m_{1/2}$-independent values of η_0 give the values of $m_{1/2}$ and $\eta_{\rm EW}$ at the minimum of the potential, as obtained from procedure (A). E.g. $\eta_0 = 8$, 10 depicted on Fig. 5, lead to $m_{1/2} \simeq 550$ GeV, $\eta_{\rm EW} \simeq .9$ and $m_{1/2} \simeq 335$ GeV, $\eta_{\rm EW} \simeq 1.1$ respectively; see also Table II. Varying η_0, one can easily read out from the general trend of the monotonically increasing η curves as compared to the monotonically decreasing critical η curve that there are basically always intersections [i.e. existence of $m_{1/2}$ minima from procedure (A)], except for too-large or too-small values of η_0. This reproduces features similar to (4.13) and (4.15) albeit here for the specific prescription $Q_{\rm EW}^{\rm default}$ for which the lower critical value of $\eta_{\rm EW}$ is around 0.7 for an $m_{1/2}$(min) around 1 TeV, as can be seen from Fig. 5. Moreover, since each η curve sweeps out all the region below the critical curve, it follows that one will always find a $m_{1/2}$ minimum solution from procedure (C) whenever there exists one from procedure (A). This is good news as it guarantees the qualitative equivalence of the two procedures even if they differ quantitatively. The situation is drastically different for the subtraction prescription. The reason is that the $\tilde{\eta}$ curves of $-V_{\rm sub}/m_{1/2}^4$ have a shape very similar to that of the corresponding critical curve, rendering the intersections rather scarce. One can see this in Fig. 5 where the green (dashed-line) curve remains very close to the critical curve (red full-line) but in fact intersects it at $m_{1/2} \simeq 210$ GeV, which is thus the outcome of procedure (A). But, after intersecting, the $-V_{\rm sub}/m_{1/2}^4$ does not go enough below the critical curve to match the 10% difference that ensures solutions from procedure (C). Indeed, we found that in this case the latter procedure does not yield any $m_{1/2}$ minimum for this specific $Q_{\rm EW}$ prescription. In fact, even for procedure (A), the minimum is found in the relatively restricted range 300 GeV $\lesssim Q \lesssim$ 500 GeV. This is not surprising in view of the almost parallel red full-line and green dashed curves, which makes the intersection more sensitive to spurious scale dependence from higher-order corrections in this prescription. Other $-m_{1/2}^{-4} V_{\rm sub}$ curves with different boundary conditions are expected to have the same behavior (see e.g. the blue curve in Fig. 5) so that one expects generically that, within the subtraction prescription, procedure (C) does not yield solutions when procedure (A) does. Thus, in contrast with the untwiddled prescription where a mere 10% effect on the minima is obtained between procedures (A) and (C), the subtraction prescription clearly provides an example where the flaws of procedure (C) become severe enough to make it qualitatively unreliable.

In summary, we learned from this section that:

(1) the subtraction prescription, although theoretically sound, does suffer from an increased sensitivity to higher-order effects making it in practice perhaps less reliable.
(2) the subtraction prescription might seem more predictive than the untwiddled prescription with the extra η_0 parameter, but this is an artifact of the specific subtraction at $H_u = H_d = 0$. In general, one can subtract at other arbitrary values of the Higgs fields with presumably different values of the minimization, thus recovering more freedom than naively expected.
(3) although, strictly speaking, only procedure (A) is correct, the comparison between the (A) and (C) procedures allowed us to better assess the impact of the various contributions (radiative corrections, physical constraints) on the determination of the minima. For instance, the effect of fixing m_Z prior to minimization in procedure (C) becomes quickly mild for increasing $m_{1/2}$, while the radiative corrections when fixing similarly $m_{\rm top}^{\rm pole}$ lead to moderate but incompressible relative differences of order 10%.
(4) the different choices of scale prescription we considered allowed us to check (within numerical uncertainties) the expected approximate one-loop scale independence of $V_{\rm full}$ and of the resulting $m_{1/2}$ minima. Also, each one of these choices can have its own practical benefit as stated previously, $Q_{\rm EW}^{\rm default}$ being the simplest in practice since readily implemented in most public codes.

In the following, we will rely exclusively on the untwiddled η prescription, namely, with $m_{1/2}$-independent η_0 at the GUT scale.

V. COLLIDER AND OTHER PHENOMENOLOGICAL CONSTRAINTS

In this section, we examine the present collider and other phenomenological constraints combined with the theoretical constraints from the requirement of nontrivial $m_{1/2}$ minima. Before going into more detail, let us start with a first lap regarding the constraints on the relevant high-scale parameters B_0 (or equivalently $\tan\beta$) and η_0. Qualitatively, as B_0 increases (here for fixed $A_0 = 0$), the occurrence of $m_{1/2}$ minima is not changing drastically, being mostly sensitive to η_0 values. But, higher B_0 implies (for fixed $A_0 = 0$) higher $B_{\rm EW}$, and correspondingly smaller $\tan\beta$ (see the discussion in Sec/ IVA and Fig. 2). Therefore, the lightest Higgs mass tends to decrease, for virtually the same $m_{1/2}$ values, with consequently a larger exclusion range in the $(m_{1/2}, \eta_0)$ parameter space. But, the present lightest Higgs bound can be accommodated even for $m_0 = 0$, provided that the $m_{1/2}$ minima are sufficiently large as can be found for specific η_0 values. More precisely, taking $\eta_0 \lesssim 8$ and $B_0 = 0.2 m_{1/2}$ one finds approximately $m_h \gtrsim 114$ GeV in agreement with present bounds [54]. Note also that a consistent B_0 input tends to favor $5 \lesssim \tan\beta \lesssim 25$, as

long as $m_{1/2} \lesssim 1$ TeV. We give for illustration in Fig. 6 the full sparticle spectrum obtained for the case $\eta_0 = 8$, $B_0 = 0.2 m_{1/2}$ (and $m_0 = A_0 = 0$) with a minimum at about $m_{1/2} \sim 500$ GeV. The lightest Higgs mass is $m_h \simeq 114.3$ GeV and this spectrum passes all other present constraints (including $b \to s\gamma$, $g_\mu - 2$, as well as the recent LHC constraints [55,56]), except for the important fact that the $\tilde{\tau}$ is the LSP. This is the case more generally in a large part of the parameter space. We shall discuss in the next section how to evade this dark matter issue by assuming that the gravitino is the true LSP and the stau the next-lightest supersymmetric particle (NLSP). The long-standing cosmological issues related to the gravitino, including gravitino LSP as a possible dark matter candidate [57], were also considered in the no-scale framework [30,58].

A. The constrained MSSM and the LSP issue

In standard mSUGRA, substantial parts of the parameter space where the lightest neutralino is the LSP and assumed to be the dark matter can be excluded by the previously established collider and relic density combined constraints [59,60]. In such a scenario, most of these results may be roughly applied in our case, provided that one superimposes on those constraints the specific $(m_{1/2}, \tan\beta)$ values theoretically constrained by the no-scale B_0 input, together with the extra constraints on the vacuum energy via η_0. This nevertheless deserves a specific study and update, as we illustrate for a few representative cases below. Now, in fact, for a large part of the relevant no-scale parameter space, the LSP is the charged stau, which is in conflict with the requirement of an electrically neutral dark matter. The neutralino mass grows faster with $m_{1/2}$ than the stau, which consequently tends to be lighter. Having a nonvanishing m_0 raises the initial value of the scalars and delays the moment where radiative contributions raise the neutralino mass, giving more easily a neutralino LSP. For rather small values of $m_{1/2}$, say less than about 300 GeV, and rather low values of $\tan\beta$, there is a window in which the neutralino and stau neutrino are lighter than the stau, but this part of the parameter space is largely excluded at present by other lower sparticle mass bounds from the LEP [54], Tevatron [61], and the latest LHC limits [55,56]. In particular, both the right selectron, the lightest chargino, and the gluino recently constrained by the LHC can easily be too light.

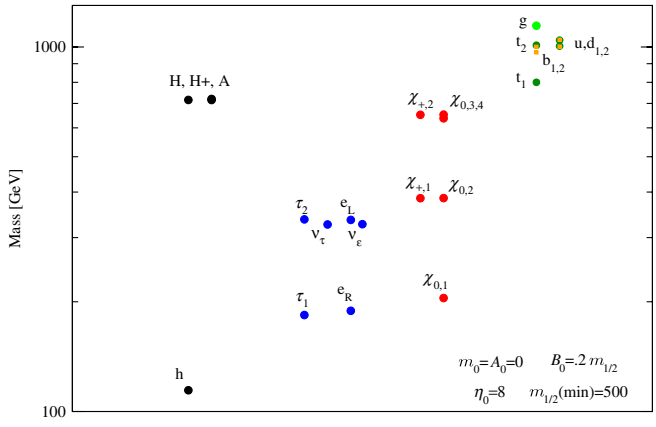

FIG. 6 (color online). A typical representative spectrum with a consistent $m_{1/2}$ minimum.

This issue can be solved by assuming that the gravitino is the true LSP, thus lighter than the stau, so that the latter is decaying to a gravitino plus a τ lepton in the early universe. In our generalized no-scale framework, the gravitino mass is required to be $\mathcal{O}(m_{1/2})$ but otherwise essentially free. For this alternative scenario, new and specific constraints arise mainly from relic density confronted with Wilkinson Microwave Anistropy Probe (WMAP) results, including also in this case the very relevant gravitino thermal contributions to the relic density.

We thus assume that the gauginos and the gravitino are linked in a manner that allows a light gravitino, though not exhibiting a precise relation. Note that the gravitino does not need to be *very* light, but just slightly below the stau and neutralino masses still with $m_{3/2}/m_{1/2} \sim \mathcal{O}(1)$. On purely phenomenological ground, we assume the simple relation (2.11) and explore the different constraints for representative choices $0.1 \lesssim c_{3/2} \lesssim 1$. More elaborate model-dependent relations are also possible [22], in particular, in superstring-derived models.

From the point of view of dark matter relic density constraints, assuming a gravitino LSP opens up a whole new area of parameters that is otherwise excluded for a neutralino LSP. Requiring in addition nontrivial no-scale $m_{1/2}$ minima and consistent B_0 input gives tighter constraints on $m_{1/2}$ and also on η_0 compatible values as we have illustrated above.

In addition, other more indirect phenomenological constraints on supersymmetric models, such as those obtained from the muon anomalous moment and the B decay observables, will be taken into account. But, indirect constraints are less drastic in general, since they can always be fulfilled by additional contributions or slightly modified scenarios, while relic density constraints are the most important from our perspective (on top of direct collider limits), since it is the only way to put constraints on the gravitino mass in this general no-scale scenario.

1. Sparticle mass limits

We use present collider limits on sparticle masses some of which are, however, model dependent. For instance, many available bounds assume a neutralino LSP, or when assuming the decay to a gravitino, that $m_{3/2}$ is very small ($m_{3/2} \lesssim 1$ keV). It is thus difficult to read out general bounds on the masses from the existing limits. For simplicity, we may apply conservatively the pre-LHC limits for the colorless MSSM particles that are strictly speaking

valid only for a mSUGRA scenario with neutralino LSP [54]:

(i) neutralino mass: $m_{\chi_1^0} > 46$ GeV; this bound could be easily evaded, however, by relaxing the gaugino unification assumption that we took for simplicity but which is by no means mandatory in a no-scale framework. Indeed, there are little theoretical constraints on the form of the gauge kinetic function, which generates a nonzero $m_{1/2}$ value, so that it may not need to be universal [22].

(ii) chargino mass: $m_{\chi_1^\pm} > 104$ GeV for $m_{\tilde{\nu}} > 200$ GeV; this lower bound can be somehow evaded in the case of a very light sneutrino (which contributes to the t-channel with destructive interference).

(iii) stau: $m_{\tilde{\tau}} > 86$–95 GeV, valid as long as ($|m_{\tilde{\tau}} - m_{\chi}| \gtrsim 7$ GeV)

(iv) smuon: $m_{\tilde{\mu}} > 95$ GeV

(v) squarks and gauginos:
Recently, CMS [55] and ATLAS [56] have put new exclusion limits on squark and gluino masses from the LHC run at 7 GeV center-of-mass energy with integrated luminosity of 35 pb^{-1}. In the mSUGRA model, this translates into lower bounds in the $m_{1/2}$–m_0 plane that are more severe from searches for multijet events than for events containing two or more leptons in the final state. Furthermore, these constraints are not very sensitive to A_0 and $\tan\beta$ as far as the latter is not very large (a regime not relevant to our case). These limits lead to a lower $m_{1/2}$ bound of about 300 GeV for moderate m_0 values 0–200 GeV. While finalizing this paper, a very recent ATLAS note [62] appeared, extending the study of jet events with missing energy for a higher luminosity of 165 pb^{-1}. This appears to exclude $m_{1/2} \lesssim 450$ GeV for low m_0 values and $A_0 = 0$ $\tan\beta = 10$, thus ruling out *a priori* our first benchmark study in Table I, if applying conservatively the limits valid for a neutralino LSP. In any case, this is not much of a problem insofar as our different benchmarks are only theoretical examples for the occurrence of no-scale minima. Note that the spectrum e.g. shown in Fig. 6 is still (slightly) above the border of present exclusions.

However, it should be emphasized that all those constraints do not necessarily apply in a large part of the parameter space considered here, where $m_{\tilde{\tau}_1} < m_{\chi_1^0}$, with a gravitino LSP and $\tilde{\tau}_1$ NLSP. Indeed, for the range of gravitino masses that we will consider, the stau NLSP is sufficiently long-lived not to produce a signal with missing energy in the detector, so that limits obtained from searches for such signals do not apply. Very recent results by ATLAS [63] dedicated to searches for long charged tracks give bounds on stable staus NLSP, $m_{\tilde{\tau}} > 136$ GeV, for a representative gauge-mediated SUSY-breaking model. Since this limit concerns a different model, its implication on no-scale would necessitate a detailed study. Nevertheless, naively fitting this $\tilde{\tau}$ mass bound for $m_0 = A_0 = 0$ and an appropriate value of $\tan\beta(B_0)$ leads to a quite similar MSSM spectrum corresponding approximately to $m_{1/2} \gtrsim 360$ GeV.

2. Higgs boson mass

Strong limits on the lightest Higgs mass are obtained from LEP and the Tevatron [54]. In fact, apart from a very small window for relatively small $m_{1/2}$, which is now essentially excluded by Tevatron and the above-mentioned very recent LHC limits, in most of the no-scale parameter space we are in the Higgs-decoupling scenario $m_A \gg m_h$ such that the standard-model-like limit on m_h essentially applies. Thus, in most of the parameter space we are considering here the LEP II constraint [54,64] should hold

$$m_h \geq 114.4 \text{ GeV}, \tag{5.1}$$

where the limit depends on $\tan\beta$ to some extent. This implies rather stringent lower bounds on $m_{1/2}$ prior to LHC squark/gluino mass limits, especially for low $\tan\beta$ (i.e. large B_0). Even for $B_0 = 0$, requiring Eq. (5.1) corresponds to $m_{1/2} \gtrsim 400$ GeV e.g. for $m_0 = A_0 = 0$. Otherwise, the most conservative limit is $m_h \geq 92.8$ GeV [54]. To take into account theoretical uncertainties, we will use a conservative limit allowing for about 3–4 GeV of theoretical uncertainties as is customary.

3. Muon anomalous moment

Supersymmetric particles can contribute at the loop level to the muon anomalous moment $a_\mu = (g-2)_\mu/2$ [65–70]. It could explain the deviation measured [71]:

$$\Delta a_\mu = a_\mu^{\text{exp}} - a_\mu^{\text{th}} = (22 \pm 10 \text{ to } 26 \pm 9) \times 10^{-10}, \tag{5.2}$$

which is about 2 to 3 standard deviations from the theoretical prediction of the standard model (for a review, see [72]).

The contributions to a_μ in no-scale models is of course a particular case of mSUGRA general contributions. These can be quite important when slepton masses are light. Corrections in a general MSSM come dominantly from loops with a chargino and a muon sneutrino and loops with a neutralino and a smuon [67]. The MSSM correction is proportional to $\tan\beta$ and its sign follows the sign of μ, thus favoring a positive sign for the μ parameter in view of (5.2). For not too large $\tan\beta$ values and choosing $\mu > 0$, one can accommodate the preferred range (5.2) for some regions of the mSUGRA parameter values compatible with no-scale models (provided of course that $m_{1/2}$ is not too large), as we shall illustrate in the next section.

4. $b \to s\gamma$

Another largely studied probe for supersymmetry is B-meson physics, in particular, the decay $b \to s\gamma$, which has been extensively measured with good accuracy and is theoretically well under control. Indeed, theoretical calculations from standard-model contributions have been now performed at the next-to-next-to-leading logarithm order [73], including also nonperturbative corrections [74]. Confronted with recent experimental measurements [54,75],

$$\mathrm{Br}(b \to s\gamma) = (3.55 \pm 0.24 \pm 0.09) \times 10^{-4}, \qquad (5.3)$$

it results in a discrepancy with the standard model slightly above 1 standard deviation, therefore potentially very constraining for new physics. The possible contributions from the MSSM are dominated by one-loop effects from chargino plus stops, and top plus charged Higgses. Next-to-leading logarithms SUSY-QCD corrections have also been calculated [76]. In mSUGRA, contributions can become sizeable for relatively large $\tan\beta$ and sufficiently small $m_{1/2}$, which is not much favored in no-scale scenarios, due to the $m_{1/2} - B_{\mathrm{EW}} - \tan\beta$ correlations inducing rather moderate $\tan\beta \lesssim 10$ values for not-too-large $m_{1/2}$ (see the discussion in Sec. IVA). We therefore anticipate that $b \to s\gamma$ constraints are relatively marginal for a large part of our no-scale inspired scenarios, especially for the strict no-scale with $m_0 = 0$.

In practice, we have used in our analysis the bounds (5.3) conservatively augmented by theoretical uncertainties as quoted e.g. in [73,74]. The precise limits are, however, not very crucial for our analysis, since as we will illustrate they give anyway (mild) constraints only for rather small $m_{1/2} \lesssim 250$–300 GeV, which, for the range of $\tan\beta$ values under consideration, are largely superseded both by the lightest Higgs mass limit from LEP and by the Tevatron and the recent LHC limits on $m_{1/2}$. (In fact, for $A_0 = 0$ and $m_0 \neq 0$ moderately small, the lightest Higgs mass bound $m_h > 114.4$ GeV generally supersedes the $b \to s\gamma$ constraints even for large $\tan\beta$ values up to $\tan\beta \simeq 40$–50, anyway unreachable in the no-scale framework. $b \to s\gamma$ can be much more constraining if $-A_0$ is large enough, $|A_0| \sim 1$–2 TeV such that the stops could be light enough, see e.g the discussion in [60]).

5. Dark matter relic density

The lightest neutralino as a candidate for dark matter has been extensively studied in many scenarios [59,60]. The part of mSUGRA parameter space giving a stau LSP should be normally excluded. This has been one argument advocating against the viability of the strict no-scale scenarios. But, if one considers a gravitino lighter than the stau, then this part of the parameter space regains interest. The gravitino dark matter candidate has also been quite studied in the past decade. In the case of gauge mediation supersymmetry breaking scenarios, this particle is naturally the LSP and was considered both for cosmological issues and in colliders signatures [77–83]. The gravitino can also be the LSP and a very interesting dark matter candidate in the context of mSUGRA scenarios [83–96].

In the present analysis, we will illustrate a few scenarios for the most representative no-scale cases as studied above. A more complete study of the constraints obtained for the full mSUGRA parameter space will be done in a forthcoming analysis, where we also consider in detail some implications and constraints from big bang nucleosynthesis on such LSP gravitino in no-scale scenario.

For the relic density, we use micrOMEGAs 2.0 [97] to compute the relic density of the neutralino or stau MSSM LSP. For scenarios with a gravitino being the real LSP (neutralino or stau being the NLSP), all supersymmetric particles decay to the NLSP well before the latter has decayed to a gravitino because all interactions to the gravitino are suppressed by the Planck mass. We first compute the relic density $\Omega_{\mathrm{NLSP}}h^2$ the NLSP would have if it did not decay to the gravitino. Then, assuming that each NLSP with mass m_{NLSP} decays to one gravitino leads to the nonthermal contribution to the gravitino relic density

$$\Omega_{3/2}^{\mathrm{NTP}}h^2 = \frac{m_{3/2}}{m_{\mathrm{NLSP}}}\Omega_{\mathrm{NLSP}}h^2, \qquad (5.4)$$

with $h = 0.73^{+0.04}_{-0.03}$ the Hubble constant in units of $100\ \mathrm{km\,Mpc^{-1}\ s^{-1}}$.

The gravitino can also be produced in scattering processes during reheating after inflation [58,98–101]. Following [99,100], the resulting gravitino yield from thermal production is controlled by the reheat temperature T_R as follows:

$$Y_{3/2}^{\mathrm{TP}}(T \ll T_R) = \sum_{i=1}^{3} y_i g_i^2(T_R)\left(1 + \frac{M_i^2(T_R)}{3m_{3/2}^2}\right) \times \ln\left(\frac{k_i}{g_i(T_R)}\right)\left(\frac{T_R}{10^{10}\ \mathrm{GeV}}\right), \qquad (5.5)$$

where i sums over gauge groups, $y_i/10^{-12} = (0.653, 1.604, 4.276)$, $k_i = (1.266, 1.312, 1.271)$, and gauge couplings and gaugino masses are calculated using the one-loop RGE. Assuming standard thermal history without release of entropy, the gravitino relic density from thermal production is

$$\Omega_{3/2}^{\mathrm{TP}}h^2 = m_{3/2}Y_{3/2}^{\mathrm{TP}}(T_0)s(T_0)h^2/\rho_c, \qquad (5.6)$$

with $\rho_c/[s(T_0)h^2] = 3.6 \times 10^{-9}$ GeV and T_0 the background temperature.

Comparing the total gravitino relic density

$$\Omega_{3/2}h^2 = \Omega_{3/2}^{\mathrm{TP}}h^2 + \Omega_{3/2}^{\mathrm{NTP}}h^2 \qquad (5.7)$$

to the one inferred from the measurements of the CMB anisotropies will constrain T_R and the MSSM parameter

space. The 3-year WMAP satellite survey has given at 3σ confidence level [102]

$$\Omega^{3\sigma}_{\rm DM}h^2 = 0.105^{+0.021}_{-0.030}. \tag{5.8}$$

B. Combined constraints

We can now combine both the theoretical no-scale constraints (i.e. the existence of nontrivial $m_{1/2}$ minima and the $B_0 - \tan\beta$ relationship) and phenomenological constraints on $m_{1/2}$ and other parameters from direct and indirect search limits at colliders and from other observables. LEP, Tevatron, and the latest LHC constraints tell us that rather low $m_{1/2}$ are now essentially excluded, and also to avoid the 114 GeV lightest Higgs limit and other indirect phenomenological and theoretical exclusions. WMAP will also give stringent constraints excluding essentially all low m_0 values (in particular the pure no-scale $m_0 = 0$ case) if the neutralino is the true LSP because the corresponding relic density comes out below the observational bound (5.8).

1. Collider and other phenomenological constraints

In Fig. 7, we give the present constraints from direct sparticle search limits and the low-energy constraints from (5.3) and (5.2), in the $(m_{1/2}, \tan\beta)$ plane for $m_0 = A_0 = 0$, most relevant to the true no-scale scenario. We do not put explicitly the above-mentioned latest LHC exclusions [55,56] on this and other subsequent plots, since these are anyway debatable given that in most of our scenarios the neutralino is not the LSP as discussed previously. A number of conclusions may be easily drawn from this figure:

(i) Because of the B_0 no-scale input, one obtains for each B_0 value specific $m_{1/2}$, $\tan\beta$ correlations. In particular, for the strict no-scale (2.10) the values of $\tan\beta$ are restricted to be $\gtrsim 20$ when taking into account other constraints. This can be consistent with the Higgs mass lower bound of $\sim$114 GeV and falls into the preferred $b \to s\gamma$ range, but in all this region of parameter space the stau is the MSSM LSP as indicated, so that a gravitino true LSP becomes a very appealing scenario.

(ii) For larger B_0 values, there can be regions where the neutralino is again the LSP, typically for $B_0 \gtrsim .15m_{1/2}$ and sufficiently small $m_{1/2}$, see the figure. But, this is generally not compatible with the light Higgs mass limit, even when allowing a large theoretical uncertainty. In principle, there could be a tiny region for such $B_0 \sim 0.2$–$0.5m_{1/2}$ values, where for sufficiently small $m_{1/2}$ one is no longer in the decoupling limit, i.e such that m_A is light enough and the bound in (5.1) no longer applies. However, in that case the very recent direct limits from the LHC [55,56] exclude virtually all of this small corner.

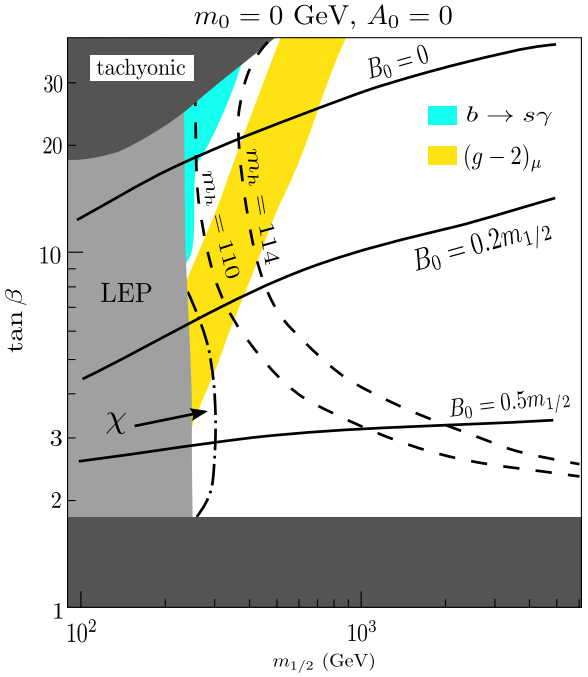

FIG. 7 (color online). Direct collider and other indirect constraints in the $(m_{1/2}, \tan\beta)$ plane for $m_0 = A_0 = 0$. The lines for three different representative B_0 input give the $m_{1/2}$–$\tan\beta$ no-scale correlations. Dark and medium grey zones indicate, respectively, the areas excluded by inconsistent REWSB ("tachyonic"), and by direct sparticle mass limits from LEP and Tevatron. The light (blue) grey zone in upper left corner is excluded by $b \to s\gamma$ constraints [75], while the (yellow) lightest grey band corresponds to values falling into the measured $g_\mu - 2$ range of (5.2). The dashed lines give the lightest Higgs mass limits and the dash-dotted line the $m_{\tilde\tau} = m_{\tilde N_1}$ border.

(iii) The requirement of nontrivial $m_{1/2}$ minima leads to constraints e.g. in the plane (B_0, η_0) or equivalently $(\tan\beta, \eta_0)$ for $m_0 = 0$, or more general ones for $m_0 \neq 0$, that we do not give explicitly. Suffice it to say that for any η_0 in the range (4.14), one can find $m_{1/2}$ minima, but present lower bounds on $m_{1/2}$ exclude accordingly $\eta_0 \gtrsim 8$–10, approximately. The most phenomenologically interesting range, obtained for not-too-large $m_{1/2} \lesssim 1$ TeV, corresponds to $5 \lesssim \eta_0 \lesssim 8$, while for smaller η_0 the corresponding $m_{1/2}$ minima increase very fast as discussed before.

2. Relic density constraints and gravitino LSP

In Fig. 8, we show the relic density values in the $(m_{1/2}, \tan\beta)$ plane corresponding to Fig. 7, calculated for $\tilde\tau$ MSSM LSP after it has decoupled from the thermal bath. We also show, in yellow, the small region where $\tilde N_1$ becomes the MSSM LSP. In the latter region, the $\tilde N_1$ abundance remains too small to be consistent with WMAP, thus excluding $\tilde N_1$ as a dark matter candidate but still allowing it

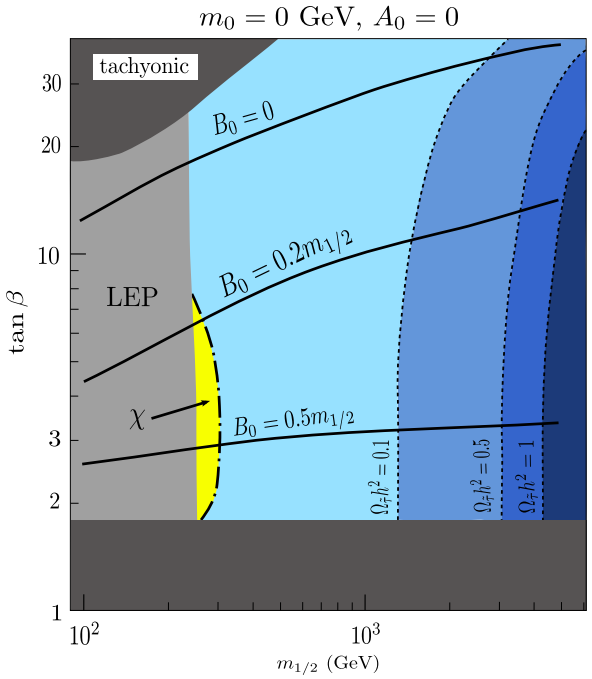

FIG. 8 (color online). $\tilde\tau$ relic density values at decoupling, in the $(m_{1/2}, \tan\beta)$ plane with $m_0 = A_0 = 0$. In all (blue) darker to lighter grey regions, $\tilde\tau$ is the MSSM LSP. Different levels of grey (blue) correspond to different values of the $\tilde\tau$ abundance, as indicated; in the specified (yellow) dash-dotted delimited region, $\tilde N_1$ becomes lighter than $\tilde\tau$ but with very small relic abundance (see text for more comments); other captions as in Fig. 7.

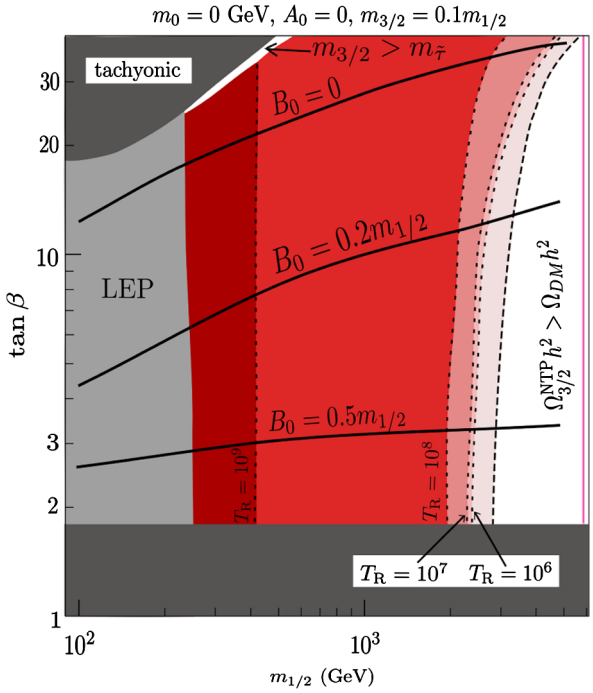

FIG. 9 (color online). Gravitino *DM* relic density values consistent with the WMAP constraints (5.8) in the $(m_{1/2}, \tan\beta)$ plane, assuming $m_{3/2} = 0.1m_{1/2}$ and $m_0 = A_0 = 0$. The different levels of (red) grey correspond to different reheat temperature values. The small region where the gravitino is not the LSP is also indicated; other captions as in Fig. 7.

as an NLSP with, in this case, a rather small nonthermal contribution to the gravitino relic density. The relic density values obtained in the (largely dominant) region where the $\tilde\tau$ is the MSSM LSP only make sense if the gravitino is the true LSP, and will lead in some parts of the parameter space to a substantial nonthermal contribution (5.4) to the total gravitino relic density. We illustrate the gravitino total relic density, obtained from (5.4) and (5.7), in Fig. 9 for $m_{3/2} = 0.1m_{1/2}$ and in Fig. 10 for a higher $m_{3/2}/m_{1/2}$ ratio, for different values of the reheating temperature T_R. The first value is such that the gravitino is the true LSP in most of the parameter space, while in the second case the unacceptable region where $m_{3/2} > m_{\tilde\tau}$ is enlarged for large $\tan\beta$. Now, one can see that it is easy to recover consistency with the WMAP relic density constraint in a large part of the parameter space, provided that T_R is sufficiently large, $T_R \gtrsim 10^6$ GeV. There are not many qualitative differences for the two illustrated $m_{3/2}$ masses. In fact, we observe that a phenomenologically most interesting case for potential early discovery at the LHC, namely, for not too large $m_{1/2} \gtrsim 400$–500, and consistency with the $g_\mu - 2$, $b \to s\gamma$ and WMAP constraints, implies a relatively large $T_R \gtrsim 10^8$–10^9 GeV, the darker red region on

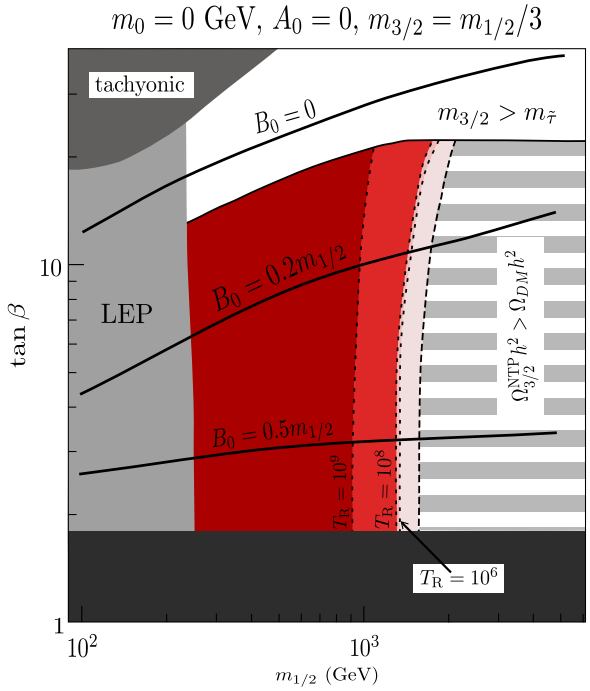

FIG. 10 (color online). Same as Fig. 9 but for $m_{3/2} = \frac{1}{3}m_{1/2}$.

the figure. A large T_R is also welcome by other independent issues such as thermal leptogenesis scenarios [103]. Indeed, a comparison of Fig. 7 and 9 shows the interesting fact that a part of the strict no-scale model $B_0 = m_0 = A_0 = 0$ is not excluded: there is a range, for $m_{1/2} \sim$ 400–800 GeV, $\tan\beta \sim 20$–25 compatible with $m_h \gtrsim$ 114 GeV, the $g_\mu - 2$ deviation (Fig. 7) and other constraints, provided the reheating temperature is 10^8–10^9 GeV.

3. Generalized no-scale scenarios

In this subsection, we consider one typical example illustrating more general cases with A_0, $m_0 \neq 0$. Since A_0 has little effect on the existence of nontrivial no-scale minima, we illustrate for simplicity here only the case $A_0 = 0$. In Fig. 11, we show the results of the same analysis as before but for $m_0 = 0.5m_{1/2}$. An important difference with the $m_0 = 0$ case in Fig. 7 is a larger region excluded by $b \to s\gamma$, which includes a substantial part of the $B_0 = 0$ line, for rather small $m_{1/2}$. Now, coming to the relic density constraints on Fig. 12 there exists an interesting region (in green) where the *neutralino*, if it is the true LSP, is compatible with WMAP. Note, however, that this region is almost entirely excluded by $b \to s\gamma$ for the $B_0 = 0$ line as can be seen on Fig. 11 and also basically excluded by the latest LHC limits on $m_{1/2}$. But, one can easily find appropriate m_0 and B_0 values such that the $b \to s\gamma$ and LHC constraints are compatible with a neutralino LSP. A full

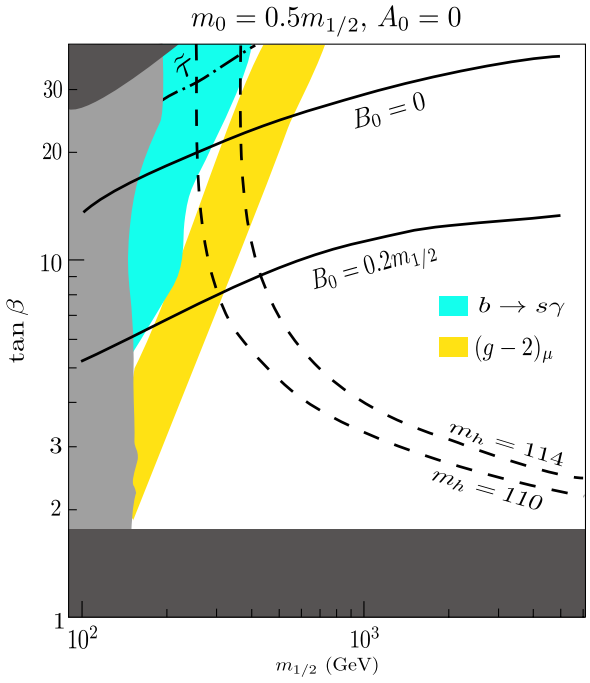

FIG. 11 (color online). Direct collider and other indirect constraints in the $(m_{1/2}, \tan\beta)$ plane for $m_0 = 0.5m_{1/2}$, $A_0 = 0$. See Fig. 7 for captions.

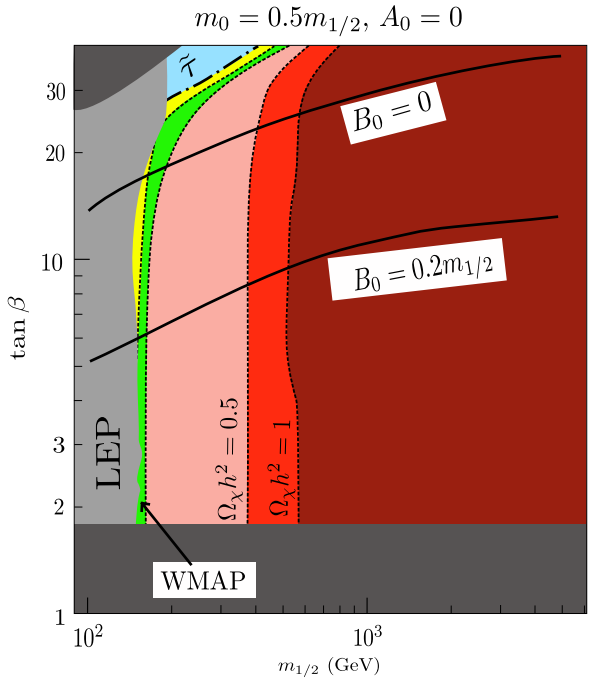

FIG. 12 (color online). Nonthermal relic density in the $(m_{1/2}, \tan\beta)$ plane for $m_0 = 0.5m_{1/2}$, $A_0 = 0$. Same captions as in Fig. 8.

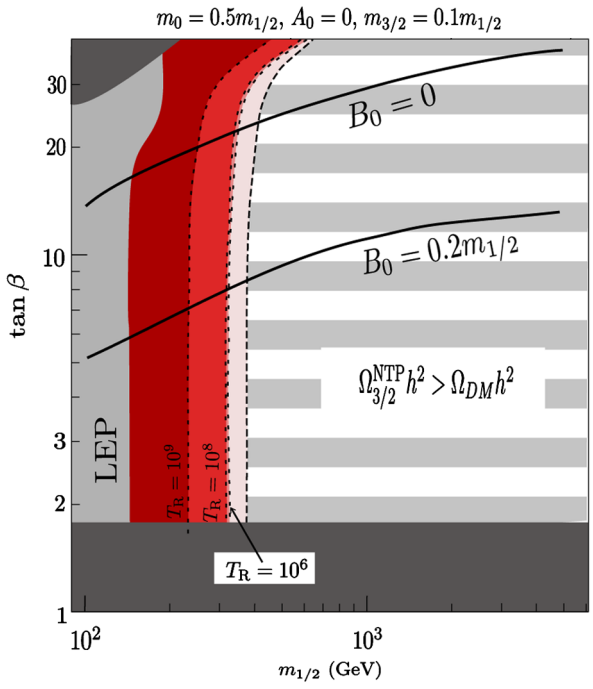

FIG. 13 (color online). Dark matter relic density values consistent with WMAP constraints (5.8) in the $(m_{1/2}, \tan\beta)$ plane, calculated assuming a gravitino $\tilde{G}$ LSP in most of the parameter space, or otherwise indicated. $m_0 = 0.5m_{1/2}$, $A_0 = 0$ and other captions as in Fig. 7. The different levels of red correspond to different reheating temperatures, as indicated.

scan of the parameter space will be explored elsewhere. Alternatively, the gravitino LSP case with its relic density is illustrated in Fig. 13, where the main difference with the $m_0 = 0$ pure no-scale case is that the consistent region with $\Omega_{3/2}^{\rm NTP} h^2 < \Omega_{\rm DM} h^2$ is shrank to much smaller $m_{1/2}$ values for which there is accordingly a tension with the latest LHC $m_{1/2}$ lower limits. For sufficiently small (but not yet all excluded) $m_{1/2}$, one can have the right relic density with a high reheating temperature almost independently of $\tan\beta$ similarly to $m_0 = 0$.

VI. CONCLUSIONS

We have reexamined generalized no-scale supergravity inspired scenarios, in which the gravitino mass and all other connected soft supersymmetry-breaking parameters can be dynamically determined through radiative corrections, triggering a nontrivial minimum of the RG-improved potential. For representative high-scale boundary conditions on the minimal supergravity model, we have examined critically the theoretical and phenomenological viability of such a mechanism in view of up-to-date calculations of the low-energy supersymmetric spectrum, taking into account all important one-loop radiative corrections. We also have investigated the impact of different prescriptions and possible variants of the minimization procedure, paying attention to the extra $m_{1/2}$ dependence, genuine or fake, induced by the implementation of physical mass constraints with various sources of radiative corrections.

We emphasize the importance of using an RG-invariant effective potential including consistently a scale-dependent vacuum energy contribution. We find that the occurrence of phenomenologically interesting minima restrict the vacuum energy to lie within a rather restricted range at the EW scale, translating into a corresponding restricted range $\Lambda_{\rm vac}^0 \sim (3\text{–}10) m_{1/2}^4$, at the GUT scale, when taking into account present LHC and other phenomenological constraints. The main practical consequences for phenomenology are to provide additional constraints on top of standard mSUGRA parameter constraints, due to the tight connection between η_0 and nontrivial $m_{1/2}$ minima, as well the $m_{1/2} - B_0 - \tan\beta$ correlations from B_0 input within the no-scale framework. Allowed regions are very restricted when considering the strict no-scale boundary conditions with $m_0 = A_0 = 0$, providing theoretical exclusion domain prior to any additional experimental constraints.

Concerning the dark matter relic density, a considerably enlarged allowed region of the mSUGRA parameter space can be obtained provided one assumes the gravitino to be the true LSP, accounting for the observed relic density with important thermal contributions. Perhaps of particular interest is the fact that the strict no-scale model $B_0 = m_0 = A_0 = 0$ is not excluded by present LHC and other experimental constraints; in particular, there is a range for $m_{1/2} \sim 400\text{–}800$ GeV, $\tan\beta \sim 20\text{–}25$ compatible with $m_h \gtrsim 114$ GeV, the $g_\mu - 2$ deviation (Fig. 7), provided the reheating temperature is $10^8\text{–}10^9$ GeV as illustrated in Fig. 9. Incidentally, this is rather close to the $(m_{1/2}, \tan\beta)$ range also preferred in recent analysis of the flipped-$SU(5)$ no-scale scenario [26]. A direct comparison of our results with the ones in these papers is however limited, since the flipped $SU(5)$ model is quite different, with modified RGEs affecting, in particular, the runnings in the gaugino sector, allowing for a neutralino LSP even for larger $m_{1/2}$ than found in our study.

Even if departing slightly from the original no-scale scenarios, the idea of dynamically fixing the soft breaking masses from extra minimization at the EW scale remains very attractive, even more so as it emphasizes the role of the vacuum energy being crucial for the occurrence of nontrivial no-scale minima. Any future experimental determination or exclusion of $m_{1/2}$ interpreted within no-scale supergravity framework will thus help pinpoint information related to the vacuum energy contribution at the EW and possibly at the GUT scale.

[1] E. Witten, Nucl. Phys. **B188**, 513 (1981).
[2] N. Sakai, Z. Phys. C **11**, 153 (1981).
[3] S. Dimopoulos and H. Georgi, Nucl. Phys. **B193**, 150 (1981).
[4] R. K. Kaul and P. Majumdar, Nucl. Phys. **B199**, 36 (1982).
[5] J. R. Ellis, S. Kelley, and D. V. Nanopoulos, Phys. Lett. B **260**, 131 (1991).
[6] U. Amaldi, W. de Boer, and H. Furstenau, Phys. Lett. B **260**, 447 (1991).
[7] P. Langacker and M.-x. Luo, Phys. Rev. D **44**, 817 (1991).
[8] C. Giunti, C. Kim, and U. Lee, Mod. Phys. Lett. A **6**, 1745 (1991).
[9] H. Goldberg, Phys. Rev. Lett. **50**, 1419 (1983).
[10] J. R. Ellis, J. Hagelin, D. V. Nanopoulos, K. A. Olive, and M. Srednicki, Nucl. Phys. **B238**, 453 (1984).
[11] G. Jungman, M. Kamionkowski, and K. Griest, Phys. Rep. **267**, 195 (1996).
[12] L. E. Ibanez and G. G. Ross, Phys. Lett. **110B**, 215 (1982).
[13] L. E. Ibanez, Phys. Lett. **118B**, 73 (1982).
[14] J. R. Ellis, D. V. Nanopoulos, and K. Tamvakis, Phys. Lett. **121B**, 123 (1983).
[15] L. Alvarez-Gaume, J. Polchinski, and M. B. Wise, Nucl. Phys. **B221**, 495 (1983).

[16] A. H. Chamseddine, R. L. Arnowitt, and P. Nath, Phys. Rev. Lett. **49**, 970 (1982).
[17] R. Barbieri, S. Ferrara, and C. A. Savoy, Phys. Lett. **119B**, 343 (1982).
[18] L. J. Hall, J. D. Lykken, and S. Weinberg, Phys. Rev. D **27**, 2359 (1983).
[19] E. Cremmer, P. Fayet, and L. Girardello, Phys. Lett. **122B**, 41 (1983).
[20] N. Ohta, Prog. Theor. Phys. **70**, 542 (1983).
[21] E. Cremmer, S. Ferrara, C. Kounnas, and D. V. Nanopoulos, Phys. Lett. **133B**, 61 (1983); J. R. Ellis, A. Lahanas, D. V. Nanopoulos, and K. Tamvakis, Phys. Lett. **134B**, 429 (1984); J. R. Ellis, C. Kounnas, and D. V. Nanopoulos, Nucl. Phys. **B241**, 406 (1984).
[22] A. Lahanas and D. V. Nanopoulos, Phys. Rep. **145**, 1 (1987).
[23] S. Ferrara, C. Kounnas, and F. Zwirner, Nucl. Phys. **B429**, 589 (1994).
[24] U. Ellwanger, Phys. Lett. B **349**, 57 (1995).
[25] B. Dutta, Y. Mimura, and D. V. Nanopoulos, Phys. Lett. B **656**, 199 (2007); J. A. Maxin, V. E. Mayes, and D. V. Nanopoulos, Phys. Rev. D **79**, 066010 (2009); J. Ellis, A. Mustafayev, and K. A. Olive, Eur. Phys. J. C **69**, 219 (2010); T. Li, J. A. Maxin, D. V. Nanopoulos, and J. W. Walker, Phys. Lett. B **699**, 164 (2011); arXiv:1105.3988.
[26] T. Li, J. A. Maxin, D. V. Nanopoulos, and J. W. Walker, Phys. Rev. D **83**, 056015 (2011); arXiv:1101.2197.
[27] C. Kounnas, F. Zwirner, and I. Pavel, Phys. Lett. B **335**, 403 (1994).
[28] S. Kelley, J. L. Lopez, D. V. Nanopoulos, and A. Zichichi, arXiv:hep-ph/9409223.
[29] G. Leontaris and N. Tracas, Phys. Lett. B **351**, 487 (1995).
[30] J. R. Ellis, K. Enqvist, and D. V. Nanopoulos, Phys. Lett. **147B**, 99 (1984); J. R. Ellis, C. Kounnas, and D. V. Nanopoulos, Phys. Lett. **143B**, 410 (1984).
[31] J. R. Ellis, C. Kounnas, and D. V. Nanopoulos, Nucl. Phys. **B247**, 373 (1984).
[32] A. Brignole, L. E. Ibanez, and C. Munoz, Nucl. Phys. **B422**, 125 (1994).
[33] C. Munoz, arXiv:hep-ph/9509290.
[34] G. Giudice and A. Masiero, Phys. Lett. B **206**, 480 (1988).
[35] S. K. Soni and H. Weldon, Phys. Lett. **126B**, 215 (1983).
[36] J. Bagger, E. Poppitz, and L. Randall, Nucl. Phys. **B426**, 3 (1994).
[37] C. Munoz, arXiv:hep-th/9507108.
[38] C. Le Mouel and G. Moultaka, Nucl. Phys. **B518**, 3 (1998).
[39] B. M. Kastening, Phys. Lett. B **283**, 287 (1992).
[40] M. Bando, T. Kugo, N. Maekawa, and H. Nakano, Phys. Lett. B **301**, 83 (1993).
[41] M. Bando, T. Kugo, N. Maekawa, and H. Nakano, Prog. Theor. Phys. **90**, 405 (1993).
[42] C. Ford, D. Jones, P. Stephenson, and M. Einhorn, Nucl. Phys. **B395**, 17 (1993).
[43] M. Sher, Phys. Rep. **179**, 273 (1989).
[44] S. R. Coleman and E. J. Weinberg, Phys. Rev. D **7**, 1888 (1973).
[45] S. P. Martin, Phys. Rev. D **66**, 096001 (2002).
[46] S. P. Martin, Phys. Rev. D **65**, 116003 (2002).
[47] M. Einhorn and D. Jones, Nucl. Phys. **B211**, 29 (1983)
[48] S. Kelley, J. L. Lopez, D. V. Nanopoulos, H. Pois, and K.-j. Yuan, Nucl. Phys. **B398**, 3 (1993).
[49] A. Djouadi, J.-L. Kneur, and G. Moultaka, Comput. Phys. Commun. **176**, 426 (2007).
[50] F. E. Paige, S. D. Protopopescu, H. Baer, and X. Tata, arXiv:hep-ph/0312045.
[51] B. Allanach, Comput. Phys. Commun. **143**, 305 (2002).
[52] W. Porod, Comput. Phys. Commun. **153**, 275 (2003).
[53] R.-J. Zhang, Phys. Lett. B **447**, 89 (1999); J. R. Espinosa and R.-J. Zhang, J. High Energy Phys. 03 (2000) 026.
[54] K. Nakamura *et al.* (Particle Data Group), J. Phys. G **37**, 075021 (2010).
[55] V. Khachatryan *et al.* (CMS Collaboration), Phys. Lett. B **698**, 196 (2011); S. Chatrchyan *et al.* (CMS Collaboration), J. High Energy Phys. 06 (2011) 026; S. Chatrchyan *et al.* (CMS Collaboration), J. High Energy Phys. 07 (2011) 113.
[56] G. Aad *et al.* (ATLAS Collaboration), arXiv:1103.6214; G. Aad *et al.* (Atlas Collaboration), Phys. Rev. Lett. **106**, 131802 (2011); arXiv:1103.4344;
[57] H. Pagels and J. R. Primack, Phys. Rev. Lett. **48**, 223 (1982); S. Weinberg, Phys. Rev. Lett. **48**, 1303 (1982); D. V. Nanopoulos, K. A. Olive, and M. Srednicki, Phys. Lett. **127B**, 30 (1983); M. Khlopov and A. D. Linde, Phys. Lett. **138B**, 265 (1984); J. R. Ellis, J. E. Kim, and D. V. Nanopoulos, Phys. Lett. **145B**, 181 (1984); R. Juszkiewicz, J. Silk, and A. Stebbins, Phys. Lett. **158B**, 463 (1985); J. R. Ellis, D. V. Nanopoulos, and S. Sarkar, Nucl. Phys. **B259**, 175 (1985); M. Kawasaki and K. Sato, Phys. Lett. B **189**, 23 (1987); V. Berezinsky, Phys. Lett. B **261**, 71 (1991).
[58] T. Moroi, H. Murayama, and M. Yamaguchi, Phys. Lett. B **303**, 289 (1993).
[59] M. Drees and M. M. Nojiri, Phys. Rev. D **47**, 376 (1993); H. Baer and M. Brhlik, Phys. Rev. D **53**, 597 (1996); J. R. Ellis, T. Falk, K. A. Olive, and M. Schmitt, Phys. Lett. B **413**, 355 (1997); J. R. Ellis, T. Falk, and K. A. Olive, Phys. Lett. B **444**, 367 (1998); A. Djouadi, M. Drees, and J. Kneur, J. High Energy Phys. 08 (2001) 055; H. Baer *et al.*, J. High Energy Phys. 07 (2002) 050; H. Baer and C. Balazs, J. Cosmol. Astropart. Phys. 05 (2003) 006; U. Chattopadhyay, A. Corsetti, and P. Nath, Phys. Rev. D **68**, 035005 (2003); J. R. Ellis, K. A. Olive, Y. Santoso, and V. C. Spanos, Phys. Lett. B **565**, 176 (2003); M. Battaglia *et al.*, Eur. Phys. J. C **33**, 273 (2004); R. L. Arnowitt, B. Dutta, and B. Hu, arXiv:hep-ph/0310103; J. R. Ellis, K. A. Olive, Y. Santoso, and V. C. Spanos, Phys. Rev. D **69**, 095004 (2004); M. E. Gomez, T. Ibrahim, P. Nath, and S. Skadhauge, Phys. Rev. D **70**, 035014 (2004); J. R. Ellis, S. Heinemeyer, K. A. Olive, and G. Weiglein, J. High Energy Phys. 02 (2005) 013; G. Belanger, S. Kraml, and A. Pukhov, Phys. Rev. D **72**, 015003 (2005)
[60] A. Djouadi, M. Drees, and J.-L. Kneur, J. High Energy Phys. 03 (2006) 033.
[61] V. Abazov *et al.* (D0 Collaboration), Phys. Lett. B **680**, 34 (2009).
[62] ATLAS Collaboration, Report No. ATLAS-CONF-2011-086, 2011.
[63] ATLAS Collaboration, arXiv:1106.4495.
[64] ALEPH, DELPHI, L3, and OPAL, Reports No. LEPSUSYWG/01-03.1 and No. 04-01.1, http://lepsusy.web.cern.ch/lepsusy/.

[65] J. L. Lopez, D. V. Nanopoulos, and X. Wang, Phys. Rev. D **49**, 366 (1994).

[66] U. Chattopadhyay and P. Nath, Phys. Rev. D **53**, 1648 (1996)

[67] T. Moroi, Phys. Rev. D **53**, 6565 (1996)

[68] M. S. Carena, G. Giudice, and C. Wagner, Phys. Lett. B **390**, 234 (1997)

[69] T. Goto, Y. Okada, and Y. Shimizu, arXiv:hep-ph/9908499.

[70] M. Drees, Y. G. Kim, T. Kobayashi, and M. M. Nojiri, Phys. Rev. D **63**, 115009 (2001)

[71] G. Bennett *et al.* (Muon G-2 Collaboration), Phys. Rev. D **73**, 072003 (2006).

[72] J. P. Miller, E. de Rafael, and B. Roberts, Rep. Prog. Phys. **70**, 795 (2007).

[73] M. Misiak *et al.*, Phys. Rev. Lett. **98**, 022002 (2007).

[74] M. Benzke, S. J. Lee, M. Neubert, and G. Paz, J. High Energy Phys. 08 (2010) 099.

[75] D. Asner *et al.* (Heavy Flavor Averaging Group), arXiv:1010.1589.

[76] G. Degrassi, P. Gambino, and G. F. Giudice, J. High Energy Phys. 12 (2000) 009; G. Degrassi, P. Gambino, and P. Slavich, Phys. Lett. B **635**, 335 (2006); Comput. Phys. Commun. **179**, 759 (2008); C. Greub, T. Hurth, V. Pilipp, C. Schupbach, and M. Steinhauser, arXiv:1105.1330.

[77] S. Ambrosanio, B. Mele, S. Petrarca, G. Polesello, and A. Rimoldi, J. High Energy Phys. 01 (2001) 014.

[78] E. A. Baltz and H. Murayama, J. High Energy Phys. 05 (2003) 067.

[79] M. Fujii and T. Yanagida, Phys. Lett. B **549**, 273 (2002).

[80] K. Kawagoe, T. Kobayashi, M. M. Nojiri, and A. Ochi, Phys. Rev. D **69**, 035003 (2004).

[81] M. Lemoine, G. Moultaka, and K. Jedamzik, Phys. Lett. B **645**, 222 (2007).

[82] K. Jedamzik, M. Lemoine, and G. Moultaka, Phys. Rev. D **73**, 043514 (2006)

[83] S. Bailly, K. Jedamzik, and G. Moultaka, Phys. Rev. D **80**, 063509 (2009).

[84] J. L. Feng, A. Rajaraman, and F. Takayama, Phys. Rev. Lett. **91**, 011302 (2003).

[85] J. L. Feng, A. Rajaraman, and F. Takayama, Phys. Rev. D **68**, 063504 (2003).

[86] J. R. Ellis, K. A. Olive, Y. Santoso, and V. C. Spanos, Phys. Lett. B **588**, 7 (2004).

[87] J. L. Feng, S. Su, and F. Takayama, Phys. Rev. D **70**, 063514 (2004).

[88] J. L. Feng, S. Su, and F. Takayama, Phys. Rev. D **70**, 075019 (2004).

[89] L. Roszkowski, R. Ruiz de Austri, and K.-Y. Choi, J. High Energy Phys. 08 (2005) 080.

[90] D. G. Cerdeno, K.-Y. Choi, K. Jedamzik, L. Roszkowski, and R. Ruiz de Austri, J. Cosmol. Astropart. Phys. 06 (2006) 005.

[91] F. D. Steffen, J. Cosmol. Astropart. Phys. 09 (2006) 001.

[92] M. Kawasaki, K. Kohri, and T. Moroi, Phys. Lett. B **649**, 436 (2007).

[93] J. Pradler and F. D. Steffen, Phys. Lett. B **666**, 181 (2008).

[94] M. Kawasaki, K. Kohri, T. Moroi, and A. Yotsuyanagi, Phys. Rev. D **78**, 065011 (2008).

[95] S. Bailly, K.-Y. Choi, K. Jedamzik, and L. Roszkowski, J. High Energy Phys. 05 (2009) 103.

[96] S. Bailly, J. Cosmol. Astropart. Phys. 03 (2011) 022.

[97] G. Belanger, F. Boudjema, A. Pukhov, and A. Semenov, Comput. Phys. Commun. **176**, 367 (2007).

[98] M. Bolz, A. Brandenburg, and W. Buchmuller, Nucl. Phys. **B606**, 518 (2001).

[99] J. Pradler and F. D. Steffen, Phys. Rev. D **75**, 023509 (2007).

[100] J. Pradler and F. D. Steffen, Phys. Lett. B **648**, 224 (2007).

[101] V. S. Rychkov and A. Strumia, Phys. Rev. D **75**, 075011 (2007).

[102] D. Spergel *et al.* (WMAP Collaboration), Astrophys. J. Suppl. Ser. **170**, 377 (2007).

[103] S. Davidson, E. Nardi, and Y. Nir, Phys. Rep. **466**, 105 (2008).